# Chapter 1
# Nanoparticles Synthesized by Microorganisms

**Abstract** Microorganisms capable of synthesizing nanoparticles are prevalent microflora of the terrestrial and marine ecosystems. These microorganisms are involved in biogeochemical cycling of metals in processes such as precipitation (biomineralization), decomposition (bioweathering), and degradation (biocorrosion). The biosynthesis of metal NPs by microbes is a function of heavy metal toxicity resistance mechanisms. Resistance mechanisms range from redox enzymes that convert toxic metal ions to inert forms, structural proteins that bind protein, or through the use of efflux proteins that transport metal ions by proton motive force, chemiosmotic gradients, or ATP hydrolysis, which work together to coordinate synthesis nanoparticle synthesis. This chapter focuses on the biological systems; bacteria, fungi, actinomycetes, and algae for utilization in nanotechnology, especially in the development of a reliable and eco-friendly processes for the synthesis of metallic nanoparticles. The rich microbial diversity points to their innate potential for acting as potential biofactories for nanoparticles synthesis.

## 1.1 Introduction

Nanoparticles (NPs) fall within the size range of 0.1–100 nm and are capable of exhibiting a range of ideal properties such as near identical strength (e.g. resistance to crushing), active surfaces, which have important catalytic properties; and discrete energy levels that can yield some important tailoring of electronic properties (Daniel and Astruc 2004; Kato 2011). While the chemical compositions of NPs are important, the morphology of the NPs (size and shape) and its surface/colloidal properties are equally essential. For example, smaller size NPs are known to have more antimicrobial activity than larger NPs (Chwalibog et al. 2010). With regard to drug delivery, the smaller the NP, the longer it will remain in the circulatory system and therefore have a greater chance of being distributed among the target sites (Gaumet et al. 2008). NPs in general can be synthetically formed or occur naturally (e.g. by microbial biosynthesis) within the environment. In both instances, variations in the morphology of the resulting NPs are common. NPs can be found as



S. Tiquia-Arashiro and D. Rodrigues, *Extremophiles: Applications in Nanotechnology*, DOI 10.1007/978-3-319-45215-9_1

nanospheres, nanorods, nanocubes, nanoplates, nanobelts, nanotetrapods, and nanoprisms. These can be loosely grouped into face-centered cubic, cuboctahedron, icosahedrons, regular decahedron, star decahedron, marks decahedron, and round decahedrons (Yacaman et al. 2001). Another extremely important aspect of NPs in addition to their morphology is their composition. For instance NPs containing metal ions have many beneficial properties, which are becoming increasingly more common in new technology and processes. For example, a recent review on silver nanoparticles (AgNP) (Sweet and Singleton 2011) covers the usage of AgNP in a wide range of applications including food storage, photonics, information storage, electronic and optical detection systems, therapeutics, diagnostics, photovoltaics, and catalysts. However, despite the significant advantages of NPs being formed with metals such as silver, the challenge of synthetically controlling the shape of metal NPs has met with variable success, making manipulation aimed at a certain size and/or shape of metal NPs difficult.

Microorganisms capable of synthesizing NPs are especially prevalent microflora of the terrestrial and marine ecosystems. It is well known that microbes are involved in biogeochemical cycles of metals in processes such as precipitation (biomineralization), decomposition (bioweathering), and degradation (biocorrosion). Central to each ecological process is the mobilization, distribution, and chemical modification that govern metal speciation and ultimately toxicity (Gadd 2010). As a consequence of these ecological processes, microbes are often subjected to toxic levels of heavy metals, which unless managed, may induce cell death. For example, silver toxicity can occur through interaction with thiol groups of membrane-bound proteins including enzymes involved in respiration, leading to disruption of the cellular membranes, and subsequent disruption of proton motive force through an inability to maintain a proton gradient. This is thought to promote uncoupling of the respiratory chain from oxidative phosphorylation, due to disruption of electron transport (Holt and Bard 2005). Uncontrolled respiration promotes superoxide and hydroxyl radical formation, leading to induction of SOS response and ultimately cell death. Similar metal toxicity responses are observed with other metals, for example, cadmium (Ahmad et al. 2002), and NP biosynthesis would appear to be a common byproduct of metal resistance. The biosynthesis of metal NPs by microbes is a function of heavy metal toxicity resistance mechanisms, whereby toxic heavy metals are converted to nontoxic species and precipitated as metal clusters of nanoscale dimension and defined shape (Narayanan and Sakthivel 2010). Resistance mechanisms range from redox enzymes that convert toxic metal ions to inert forms, structural proteins that bind protein (Gadd 2010), or through the use of efflux proteins that transport metal ions by proton motive force, chemiosmotic gradients, or ATP hydrolysis (Nies 2003). It is proposed that such mechanisms work to coordinate synthesis. This chapter provides an overview of the different types of NPs and the different microorganisms that synthesize them.

The general scheme of the formation of metallic nanoparticles through biosynthesis is shown in Fig. 1.1. The nanoparticles are produced either intracellularly or

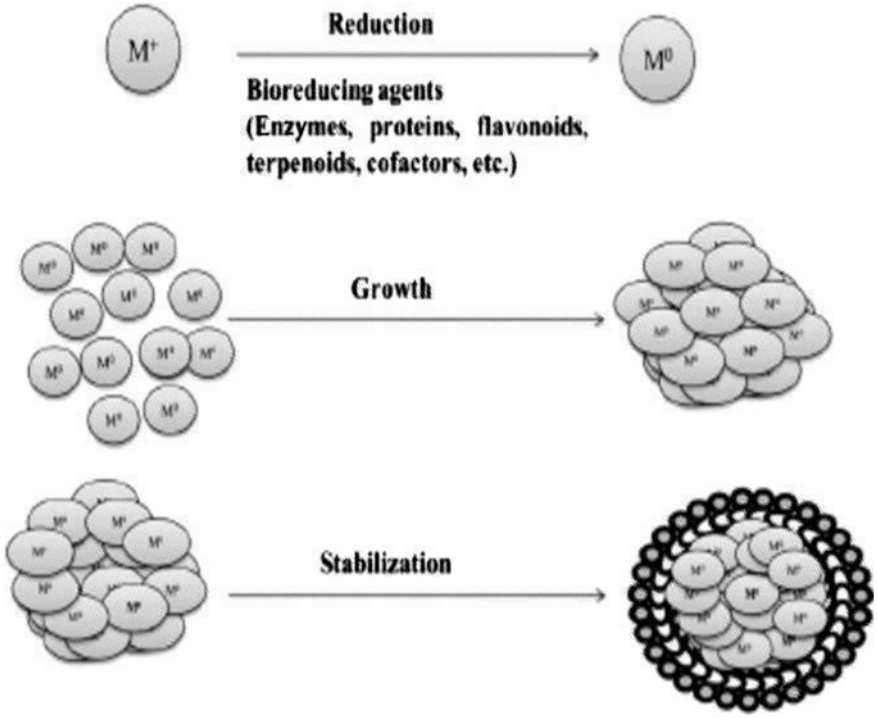


**Fig. 1.1** The formation of the metal nanoparticles (Me-NPs) during biosynthesis. *Source* Mittal et al. (2013). Copyright © 2013, Elsevier. Reproduced with permission

extracellularly (Rangarajan et al. 2014). In case of the intracellular synthesis the nanoparticles are produced inside the bacterial cells by the reductive pathways of the cell wall and accumulated in the periplasmic space of the cell. The nanoparticles are produced extracellularly when the cell wall reductive enzymes or soluble secreted enzymes are extracted outside the cell and are involved in the reductive process of metal ions.

One of the enzymes involved in the biosynthesis of metal nanoparticles is the nitrate reductase which reduces the metal ions ($Me^{+1}$) to the metallic form ($Me^{0}$). This enzyme is a NADH- and NADPH-dependent enzyme. He et al. (2007) described the hypothetical mechanism for gold nanoparticles biosynthesis carried out by *Rhodopseudomonas capsulate*. These bacteria are known to secrete cofactor NADH- and NADH-dependent enzymes that can be responsible for the biological reduction of $Au^{3+}$ to $Au^{0}$ and the subsequent formation of gold nanoparticles (Fig. 1.2). This reduction is initiated by electron transfer from the NADH by NADH-dependent reductase as electron carrier during which the gold ions gain electrons and are therefore reduced to $Au^{0}$.

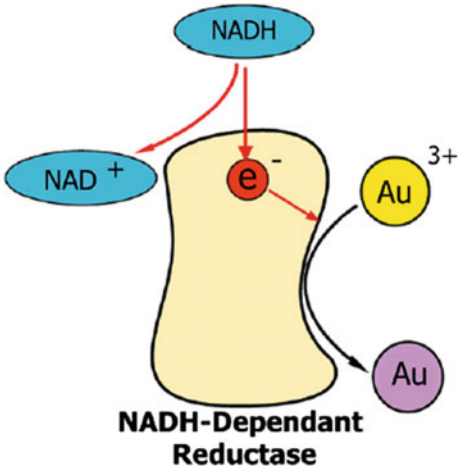


**Fig. 1.2** Hypothetical mechanism for silver and gold nanoparticles biosynthesis. *Source* He et al. (2007). Copyright © 2007, Elsevier. Reproduced with permission

## 1.2 Metallic Nanoparticles

Metallic nanoparticles have fascinated scientist for over a century and are now heavily utilized in biomedical sciences and engineering. They are a focus of interest because of their huge potential in nanotechnology. Metallic nanoparticles have possible applications in diverse areas such as electronics, cosmetics, coatings, packaging, and biotechnology. For example, nanoparticles can be induced to merge into a solid at relatively lower temperatures, often without melting, leading to improved and easy-to-create coatings for electronics applications. Typically, NPs possess a wavelength below the critical wavelength of light. This renders them transparent, a property that makes them very useful for applications in cosmetics, coatings, and packaging. Metallic NPs can be attached to single strands of DNA nondestructively. This opens up avenues for medical diagnostic applications. Nanoparticles can traverse through the vasculature and localize any target organ. This potentially can lead to novel therapeutic, imaging, and biomedical applications. Today these materials can be synthesized and modified with various chemical functional groups which allow them to be conjugated with antibodies, ligands, and drugs of interest and thus opening a wide range of potential applications in biotechnology, magnetic separation, and preconcentration of target analytes, targeted drug delivery, and vehicles for gene and drug delivery and more importantly diagnostic imaging (Mody et al. 2010). Some typical metal nanoparticles produced by microorganisms are summarized in Table 1.1.

**Table 1.1** Metal nanoparticles synthesized by microorganisms

| Microorganism | Type nanoparticle synthesize | Size (nm) | Shape | Reference |
|---|---|---|---|---|
| **Bacteria** | | | | |
| *Actinobacter* spp. | Magnetite | 10–40 | Not available | Bharde et al. (2005) |
| *Bacillus lichineformis* | Silver | 50 | Not available | Kalimuthu et al. (2008) |
| *Bacillus cereus* | Silver | 4–5 | Spherical | Babu and Gunasekaran (2009) |
| *Brevibacterium casei* | Gold, silver | 10–50 | Spherical | Kalishwaralal et al. (2010) |
| *Clostridium thermoaceticum* | Cadmium sulfide | Not available | Not available | Sweeney et al. (2004) |
| *Corynebacterium glutamicum* | Silver | 5–50 | Irregular | Gurunathan et al. (2009) |
| *Desulfovibrio desulfuricans* | Palladium | 50 | Spherical | Lloyd et al. (1998) |
| *Enterobacter* sp. | Mercury | 2–5 | Spherical | Sinha and Khare (2011) |
| *Escherichia coli* | Gold | 20–30 | Triangles, hexagons | Gericke and Pinches (2006) |
| *Escherichia coli* | Cadmium telluride | 2-3 | Spherical | Bao et al. (2010) |
| *Klebsiella pneumoniae* | Gold | 5–32 | Not available | Malarkodi et al. (2013) |
| *Lactobacillus* spp. | Gold, Silver | Not available | Not available | Nair and Pradeep (2002) |
| *Pseudomonas aeruginosa* | Gold | 15–30 | Not available | Husseiny et al. (2007) |
| *Pseudomonas stutzeri* | Silver | 200 nm | Not available | Klaus et al. (1999) |
| *Pyrobaculum islandicum* | Uranium (VI), Technetium (VII), Chromium (VI), Cobalt (III), Manganese (IV) | Not available | Spherical | Kashefi and Lovley (2000) |
| *Rhodococcus* sp. | Gold | 5–15 | Spherical | Ahmad et al. (2003b) |
| *Rhodopseudomonas capsulate* | Gold | 10–20 | Spherical | He et al. (2007) |
| *Shewanella algae* | Gold | 10–20 | Not available | Konishi et al. (2007a) |
| *Shewanella oneidensis* | Gold | 12–17 | Spherical | Suresh et al. (2011) |
| *Shewanella algae* | Platinum | 5 | Not available | Konishi et al. (2007b) |

(continued)

**Table 1.1** (continued)

| Microorganism | Type nanoparticle synthesize | Size (nm) | Shape | Reference |
|---|---|---|---|---|
| *Shewanella* sp. | Selenium | 181–221 | Spherical | Lee et al. (2007) |
| *Thermonospora* | Silver | 8 | Not available | Ahmad et al. (2003a) |
| *Ureibacillus thermosphaericus* | Silver | 50–70 | Not available | Juibari et al. (2011) |
| **Fungi** | | | | |
| *Aspergillus flavus* | Silver | 8–9 | Spherical | Vigneshwaran et al. (2007) |
| *Aspergillus fumigatus* | Silver | 5–25 | Spherical | Bhainsa and D'Souza (2006) |
| *Candida utilis* | Gold | Not available | Not available | Gericke and Pinches (2006) |
| *Fusarium oxysporum* | Silver | 5–50 | Spherical | Senapati et al. (2004) |
| *Fusarium oxysporum* | Silicon | 5–10 | Spherical | Bansal et al. (2005) |
| *Fusarium oxysporum* | Titanium | 6–13 | Spherical | Bansal et al. (2005) |
| *Neurospora crassa* | Gold, silver/gold | 32, 20–50 | Spherical | Castro-Longoria et al. (2011) |
| *Phaenerochaete chrysosporium* | Silver | 50–200 | Pyramidal | Vigneshwaran et al. (2006) |
| *Trichoderma viride* | Silver | 5–40 | Spherical | Fayaz et al. (2010) |
| *Verticillium luteoalbum* | Gold | Not available | Not available | Gericke and Pinches (2006) |
| *Verticillium* sp. | Silver | 25–32 | Spherical | Senapati et al. (2004) |
| *Yarrowia lipolytica* | Gold | 15 | Triangles | Agnihotri et al. (2009) |
| **Algae** | | | | |
| *Chlorella vulgaris* | Silver | 9–20 | Not available | Jianping et al. (2007) |
| *Oscillatoria willei* | Silver | 100–200 | Spherical | Mubarak-Ali et al. ( 2011) |
| *Plectonemaboryanum* | Gold | <10–25 | Cubic | Lengke et al. (2006a) |
| *Plectonema boryanum* UTEX 485 | Gold | 10–6 μm | Octahedral | Lengke et al. (2006b) |
| *Sargassum wightii* | Gold | 8–12 | Planar | Singaravelu et al. (2007) |

(continued)

**Table 1.1** (continued)

| Microorganism | Type nanoparticle synthesize | Size (nm) | Shape | Reference |
|---|---|---|---|---|
| *Spirulina platenensis* | Silver | 11.6 | Spherical | Mahdieh et al. (2012) |
| *Pterochladia capillacae* | Silver | 7 (average) | Spherical | El-Rafie et al. (2013) |
| *Jania rubins* | Silver | 12 (average) | Spherical | El-Rafie et al. (2013) |
| *Ulva faciata* | Silver | 7 (average) | Spherical | El-Rafie et al. (2013) |
| *Colpmenia sinusa* | Silver | 20 (average) | Spherical | El-Rafie et al. (2013) |

### *1.2.1 Gold Nanoparticles*

Gold nanoparticles (AuNOs) have attracted attention in biotechnology due to their unique optical and electrical properties, high chemical and thermal ability, and good biocompatibility and potential applications in various life sciences related applications including biosensing, bioimaging, drug delivery for cancer diagnosis and therapy (Jiang et al. 2012). Covalently modified gold nanoparticles have attracted a great deal of interest as a drug delivery vehicles. Their predictable and reliable surface modification chemistry, usually through gold-thiol binding, makes the desired functionalization of nanoparticles quite possible and accurate. A variety of therapeutic molecules have been attached in this manner, including various oligonucleotides for gene therapy, bacterial compounds, and anti-cancer drugs. (Jiang et al. 2012). Recently, many advancements were made in biomedical applications with better biocompatibility in disease diagnosis and therapeutics. AuNPs could be prepared and conjugated with many functionalizing agents, such as polymers, surfactants, ligands, dendrimers, drugs, DNA, RNA, proteins, peptides and oligonucleotides. Overall, Au-NPs would be a promising vehicle for drug delivery and therapies. AuNPs can be produced by microorganisms such as bacteria, fungi and algae (Table 1.1).

Bacteria have been used to synthesize AuNPs. For example, microbial synthesis of gold nanoparticles was achieved by Konishi et al. (2007a) using the mesophilic bacterium *Shewanella algae* with $H_2$ as the electron donor. The authors used varying pH conditions in their study. When the solution pH was 7, gold nanoparticles of 10–20 nm were synthesized in the periplasmic space of *S. algae* cells. Interestingly, when the solution pH was decreased to 1, larger-sized gold nanoparticles (50–500 nm) were precipitated extracellularly (Konishi et al. 2004). In an analogous study, He et al. (2007) showed that the bacteria *Rhodopseudomonas capsulata* produces gold nanoparticles of different sizes and shapes. He et al. incubated *R. capsulata* biomass and aqueous chloroauric acid ($HAuCl_4$) solution at pH values ranging from 7 to 4.16 They found that at pH 7, spherical gold nanoparticles in the

range of 10–20 nm were formed. In contrast, at pH 4, a number of nanoplates were produced (He et al. 2007). In both of these studies, the solution pH was an important factor in controlling the morphology of biogenic gold particles and location of gold deposition. These observations are in line with the findings of Klaus et al. (1999) who observed that variations in incubation conditions lead to variations in particle size. Of note, gold nanoparticles can be used for a variety of applications (e.g., direct electrochemistry of proteins) (Liangwei et al. 2007). The synthesis of gold nanoparticles by two novel strains of *Arthrobacter* sp. 61B and *Arthrobacter globiformis* 151B isolated from basalt rocks in Georgia was studied by Kalabegishvili et al. (2012). Their study has shown that the extracellular formation of nanoparticles took place after 1.5–2 days. They noted that the concentration of gold particles accumulated by increases in bacterial biomass. Gericke and Pinches (2006) reported intracellular gold production by *Pseudomonas stutzeri* NCIMB 13420, *Bacillus subtilis* DSM 10 and *Pseudomonas putida* DSM 291. He et al. (2007) demonstrated that the bacterium *Rhodopseudomonas capsulata* is capable of producing gold particles extracellularly. The gold nanoparticles produced are stable in solution. In the study conducted by Malarkodi et al. (2013), the extracellular biosynthesis of gold nanoparticles is achieved by an easy biological procedure using *Klebsiella pneumoniae* as the reducing agent. After exposing the gold ions to *K. pneumoniae,* rapid reduction of gold ion is observed and leads to the formation of gold nanoparticles in colloidal solution (Figs. 1.3 and 1.4). The method exploits a

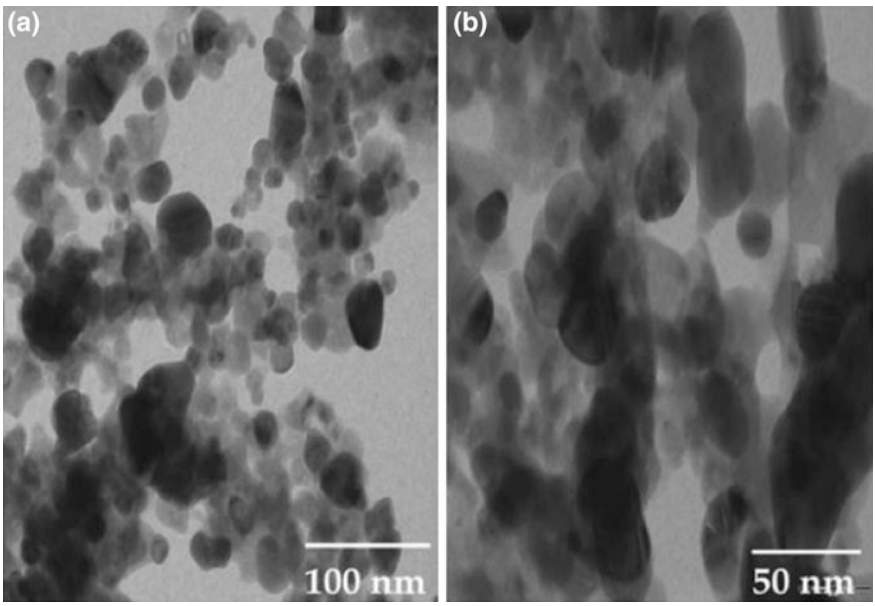


**Fig. 1.3** Transmission electron microscopy and photo of gold nanoparticles prepared by using *K. pneumoniae* **a** 100 nm and **b** 50 nm. TEM images of gold nanoparticles using *K. pneumoniae* **a** and **b**. *Source* Malarkodi et al. (2013). Copyright © 2013, Springer. Reproduced with permission

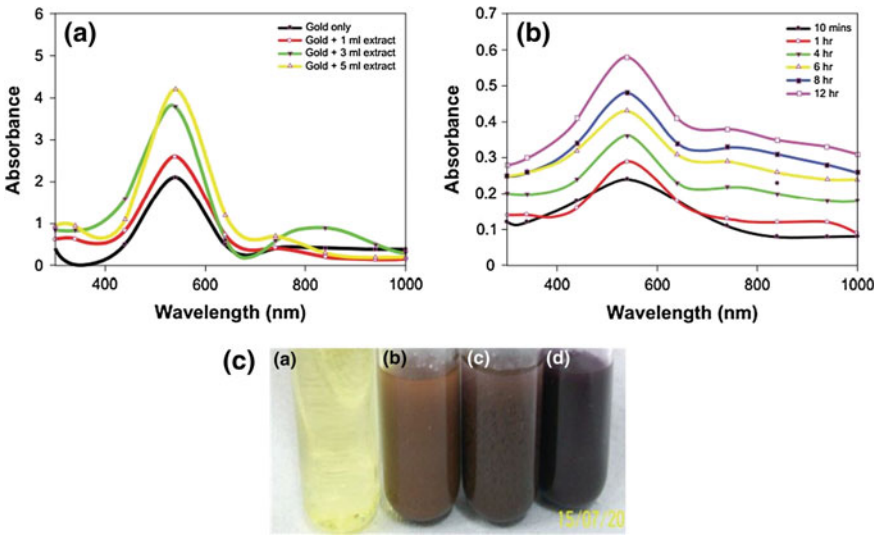


**Fig. 1.4** **a** Ultraviolet-visible-near infrared spectra of gold nanoparticles synthesized by exposing various amounts of *Candida albicans* cytosolic extract to a fixed volume (5 mL) of $HAuCl_4$ solution (10–3 M), keeping the final volume (10 mL) of reaction mixture for 24 h. **b** Representative ultraviolet-visible-near infrared spectra depicting kinetics of the reaction of 1 mL of *C. albicans* cytosolic extract with 10 mL of aqueous $HAuCl_4$ solution for specified time periods. The incubation mixture was scanned in the ultraviolet range to analyze characteristic peaks. **c** Color development as a function of surface plasmon resonance in *C. albicans* cytosolic extract-mediated synthesis of gold nanoparticles. (*a*) $HAuCl_4$ aqueous solution, (*b*) Incubation of 5 mL of $HAuCl_4$ aqueous solution with 1 mL of *C. albicans* cytosolic extract keeping the final volume of reaction mixture at 10 mL, (*c*) Incubation of $HAuCl_4$ aqueous solution (5 mL) with 3 mL of *C. albicans* cytosolic extract, making the final volume of reaction mixture 10 mL by adding 2 mL of deionized water, (*d*) 5 mL of *C. albicans* cytosolic extract incubated with 5 mL of aqueous $HAuCl_4$ solution. *Source* Chauhan et al. (2011). Copyright © 2011, Dovepress. Reproduced with permission

cheap and easily available biomaterial for the synthesis of metallic nanoparticles (Malarkodi et al. 2013).

Fungi are taking the center stage of studies on biological generation of metallic nanoparticles because of their tolerance and metal bioaccumulation ability (Sastry et al. 2003). A distinct advantage of using fungi in nanoparticle synthesis is the ease in their scale-up (e.g., using a thin solid substrate fermentation method). Given that fungi are extremely efficient secretors of extracellular enzymes, it is thus possible to easily obtain large-scale production of enzymes. Further advantages of using a fungal-mediated green approach for synthesis of metallic nanoparticles include economic viability and ease in handling biomass. However, a significant drawback of using these bio-entities in nanoparticles synthesis is that the genetic manipulation of eukaryotic organisms as a means of overexpressing specific enzymes (e.g. the ones identified in synthesis of metallic nanoparticles) is relatively much more difficult than that in prokaryotes. Sastry and coworkers have reported the

extracellular synthesis of gold nanoparticles by fungus *Fusarium oxysporum* (Mukherjee et al. 2002). They reported the intracellular synthesis of gold nanoparticles by fungus *Verticillium* sp. as well (Mukherjee et al. 2001a). The extracellular and intracellular biosynthesis of gold nanoparticles by fungus *Trichothecium* sp. was reported by Absar et al. (2005). The gold ions react with the *Trichothecium* sp. fungal biomass under stationary conditions, resulting in the rapid extracellular production of nanoparticles; reaction of the biomass under shaking conditions resulted in intracellular production of the gold nanoparticles. Chauhan et al. (2011) reported biogenic synthesis of gold nanoparticles using cytosolic extract of *Candida albicans*. The study revealed that the shape and the size of nanoparticles formed govern the characteristic features of their spectra (Figs. 1.5 and 1.6). This technique can be extended for rapid, specific, and cost-effective detection of various cancers, hormones, pathogenic microbes, and their toxins if a specific antibody is available.

There are few reports of algae being used as a "biofactory" for synthesis of metallic nanoparticles. Singaravelu et al. (2007) adopted a systematic approach to study the synthesis of metallic nanoparticles by *Sargassum wightii.* This is the first

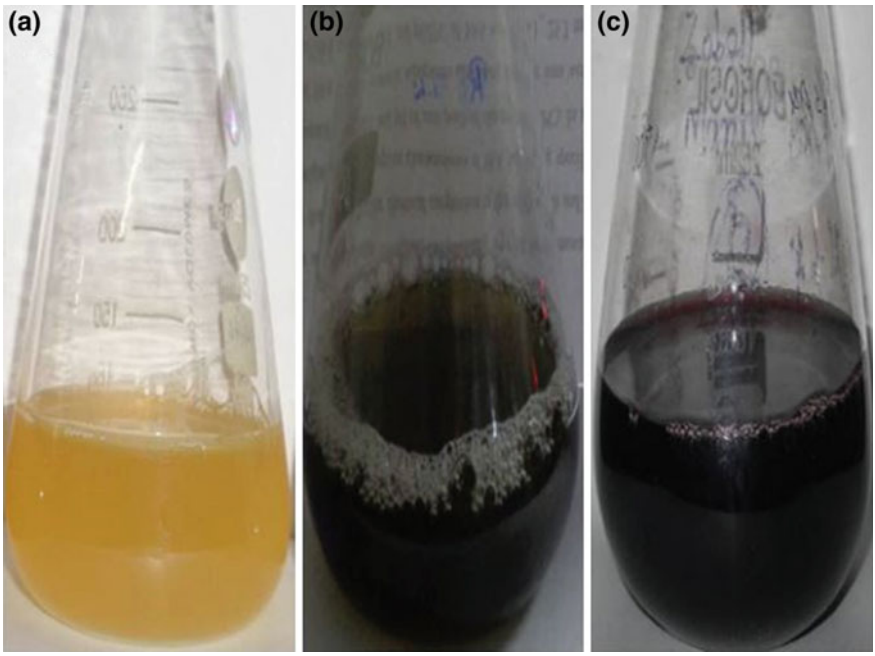


**Fig. 1.5** Extracellular synthesis of *K. pneumoniae* biomass and gold chloride mixed with biomass. *K. pneumoniae* biomass (**a**), 1 mM gold chloride mixed with biomass at the beginning of reaction showing a greenish-brown color change (**b**), and after 1 day of reaction showing a dark-purple in color change (**c**). *Source* Malarkodi et al. (2013). Copyright © 2013, Springer. Reproduced with permission

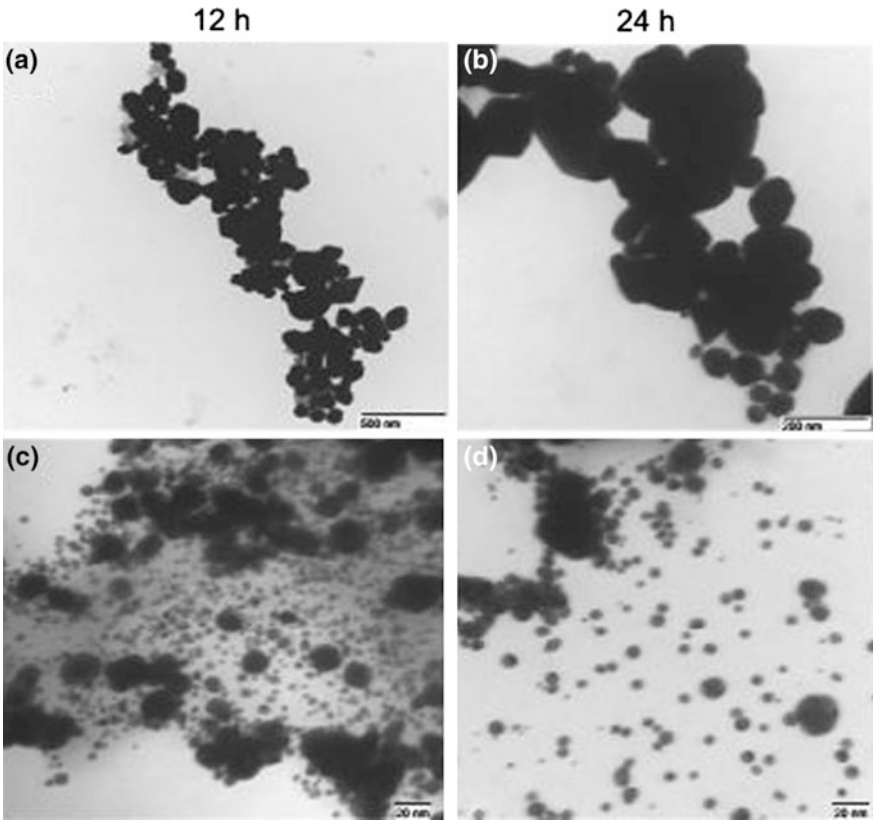


**Fig. 1.6** Representative transmission electron micrographs of gold nanoparticles synthesized using various amounts of *Candida albicans* cytosolic extract. Transmission electron micrographs of gold nanoparticles generated upon incubation of 5 mL of $HAuCl_4$ (10−3 M) with 1 mL of *C. albicans* cytosolic extract and making up final volume of reaction mixture (10 mL) using deionized water for **a** 12 h and **b** 24 h. **c** and **d** represent transmission electron microscopic images of nanoparticles obtained as a result of reduction of 5 mL of $HAuCl_4$ solution (10−3 M) by 5 mL of cytosolic extract after 12 h and 24 h, respectively. *Source* Chauhan et al. (2011). Copyright © 2011, Dovepress. Reproduced with permission

report in which a marine alga has been used to synthesize highly stable extracellular gold nanoparticles in a relatively short time period compared with that of other biological procedures. Indeed, 95 % of the bioreduction of $AuCl^{-4}$ ions occurred within 12 h at stirring condition (Singaravelu et al. 2007). The authors extended their report to the formation of palladium and platinum nanoparticles starting with their corresponding metallic chloride—containing salts (Singaravelu et al. 2007). Rajeshkumar et al. (2013, 2014) reported synthesis of gold particles by marine brown algae *Tubinaria conoides*. The nanoparticles showed antibacterial activity against *Streptococcus* sp., *Bacillus subtilis*, *Klebsiella pneumoniae*.

Southam and Beveridge (1996) have demonstrated that gold particles of nanoscale dimensions may readily be precipitated within bacterial cells by incubation of the cells with $Au^{3+}$ ions. Monodisperse gold nanoparticles have been synthesized by using alkalotolerant *Rhodococcus* sp. under extreme biological conditions like alkaline and slightly elevated temperature conditions (Ahmad et al. 2003b). Lengke et al. (2006a) claimed the synthesis of gold nanostructures in different shapes (spherical, cubic, and octahedral) by filamentous cyanobacteria from Au(I)-thiosulfate and Au(III)-chloride complexes and analyzed their formation mechanisms (Lengke et al. 2006a, b). Nair and Pradeep (2002) reported the growth of nanocrystals and nanoalloys using *Lactobacillus*. Some other typical gold nanoparticles produced by microorganisms are summarized in Table 1.1.

### *1.2.2 Silver Nanoparticles*

Silver nanoparticles (AgNps), like their bulk counterpart, show effective antimicrobial activity against Gram-positive and Gram-negative bacteria, including highly multiresistant strains such as methicillin-resistant *Staphylococcus aureus* (Panacek et al. 2006). Silver nanoparticles synthesis by microorganisms is a result of their defense mechanism. The resistance caused by the microorganism for silver ions in the environment is responsible for its nanoparticle synthesis. The silver ions in nature are highly toxic to microorganisms. As a defense mechanism, the microorganism utilizes its cellular machinery to transform the reactive silver ions to stable silver atoms. Parameters such as temperature and pH play an important role in their production. It is now known that more nanoparticles are synthesized under alkaline conditions than under acidic conditions (Saklani and Jain 2012).

The reduction of $Ag^+$ to colloidal silver by microorganisms in aqueous solutions is a stepwise process. First various complexes of $Ag^+$ are reduced to metallic silver atoms ($Ag^0$). This is followed by the agglomeration of $Ag^0$ into oligomeric clusters (Sharma et al. 2008). It is these clusters that eventually lead to the formation of colloidal AgNPs (Kapoor et al. 1994; Sharma et al. 2008). The low molecular weight peptide, glutathione (GSH) and proteins like metallothioneins and phytochelatins, enzymes such as oxidoreductases, NADH-dependent reductases, nitroreductases, NADH-dependent nitrate reductases (NRs) and cysteine desulfhydrases have been shown to be responsible for nanocrystal formation in yeast, bacteria, and fungi. These microbes are known to reduce the $Ag^+$ ions to form silver nanoparticles, most of which are found to be spherical particles (Mukherjee et al. 2001b; Ahmad et al. 2003a; Fayaz et al. 2010). In one of the earliest studies in this technology, Slawson et al. (1992) found that a silver-resistant bacterial strain isolated from silver mines, *Pseudomonas stutzeri* AG259, accumulated AgNPs within the periplasmic space. Of note, the particle size ranged from 35 to 46 nm (Slawson et al. 1992). Interestingly, Klaus et al. (1999) observed that when this bacterium was placed in concentrated aqueous solution (50 mM), particles of larger size (200 nm) were formed. Klaus et al. (1999) group attributed the difference in

particle size (in comparison with the report of Slawson et al. 1992) to the differences in cell growth and metal incubation conditions. Klaus et al. (1999) have shown that the bacterium *Pseudomonas stutzeri* AG259, isolated from a silver mine, when placed in a concentrated aqueous solution of silver nitrate, played a major role in the reduction of the $Ag^+$ ions and the formation of silver nanoparticles (AgNPs) of well-defined size and distinct topography within the periplasmic space of the bacteria (Klaus et al. 1999). An important application of such a bacterium would be in industrial Ag recovery. Intriguingly, the exact mechanism(s) of AgNPs synthesis by this bacterium is still unclear. However, the molecular basis of biochemical synthesis of AgNPs from *Morganella* sp. RP-42, an insect midgut isolate (Parikh et al. 2008). Parikh et al. (2008) observed that *Morganella* sp. RP-42 when exposed to silver nitrate ($AgNO_3$) produced extracellular crystalline AgNPs of size $20 \pm 5$ nm. Three gene homologues (*sil*E, *sil*P, and *sil*S) were identified in silver-resistant *Morganella* sp. The homologue of *sil*E from *Morganella* sp. showed 99 % nucleotide sequence similarity with the previously reported gene, *sil*E, which encodes a periplasmic silver-binding protein (Parikh et al. 2008). This is the only report that elucidates the molecular evidence of silver resistance in bacteria, which could be linked to synthesis mechanism. In another study, Nair and Pradeep (2002), exposed common *Lactobacillus* strains present in buttermilk to large concentrations of metal ions to produce microscopic gold, silver, and gold-silver alloy crystals of well-defined morphology. The bacteria produced these intracellularly and, remarkably, the cells preserved their viability even after crystal growth (Nair and Pradeep 2002) Notably, even cyanobacteria have been observed to produce AgNPs. For example, the biosynthesis of AgNPs has been successfully conducted using *Plectonema boryanum* UTEX 485, a filamentous cyanobacterium (Lengke et al. 2007). The authors posit that the mechanisms of AgNPs production via cyanobacteria could involve metabolic processes from the use of nitrate at 25 °C and/or organics released from the dead cyanobacteria at 25° (Fig. 1.7) to 100 °C (Fig. 1.8).

AgNPs were synthesized in the form of a film or produced in solution or accumulated on the cell surface of fungi, *Verticillium*, *Fusarium oxysporum*, or *Aspergillus flavus*, were employed (Mukherjee et al. 2001b; Senapati et al. 2004; Bhainsa and D'Souza 2006; Vigneshwaran et al. 2007; Jain et al. 2011). Mukherjee et al. (2001b) studied the synthesis of intracellular AgNPs using the fungus *Verticillium.* The authors observed that exposure of the fungal biomass to aqueous $Ag^+$ ions results in the intracellular reduction of the metal ions and formation of $25 \pm 12$ nm AgNPs. A shortcoming of the study by Mukherjee et al. (2001b) was that the metallic nanoparticles were synthesized intracellularly. Indeed, when the site of nanoparticle synthesis is intracellular, downstream processing becomes difficult and often defeats the purpose of developing a simple and cheap process. In this regard, Bhainsa and D'Souza (2006) have reported extracellular biosynthesis of AgNPs using the filamentous fungus *Aspergillus fumigatus* and the synthesis process was rapid. AgNPs were formed within minutes of silver ion coming in contact with the cell filtrate. The ultraviolet-visible (UV-Vis) spectrum of the aqueous medium containing $Ag^+$ ion showed a peak at 420 nm corresponding with

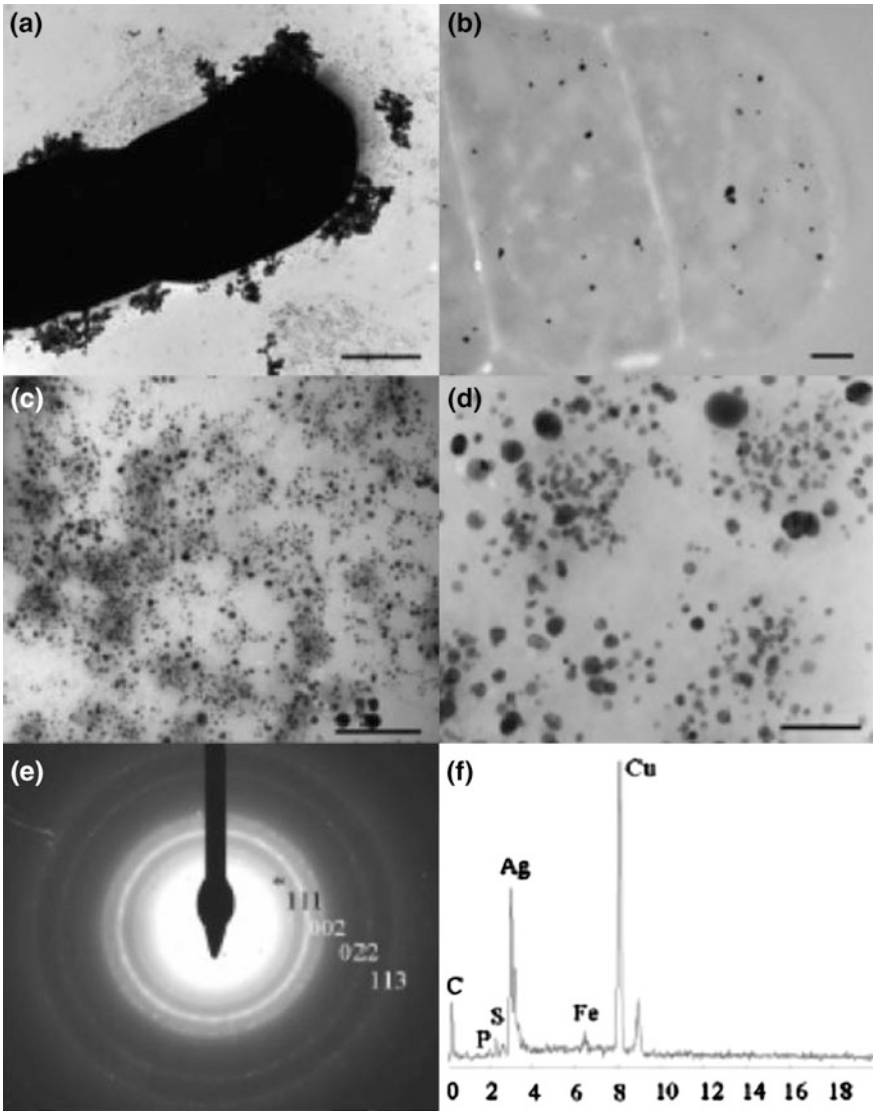


**Fig. 1.7** TEM micrographs of whole mounts of cyanobacterial cells cultured in the presence of $AgNO_3$ at 25 °C and 28 days. **a** Precipitation of silver nanoparticles on the cyanobacterial surface. **b** TEM micrograph of a thin section of cyanobacteria cells with nanoparticles of silver deposited inside the cell. **c**, **d** Spherical nanoparticles of silver precipitated in solution. **e** TEM-SAED diffraction powder-ring pattern consistent with crystalline nanoparticles of Ag with a possible trace of silver sulfide (*). *d* spacings of 0.235, 0.204, 0.144, and 0.123 nm corresponding to reflections 111, 200, 220, and 311, respectively. **f** TEM-EDS for area D. Scale bars in A, B, C, and D are 0.5 and 0.2 nm and 25 and 50 nm, respectively. *Source* Lengke et al. (2007). Copyright © 2007, American Chemical Society. Reproduced with permission

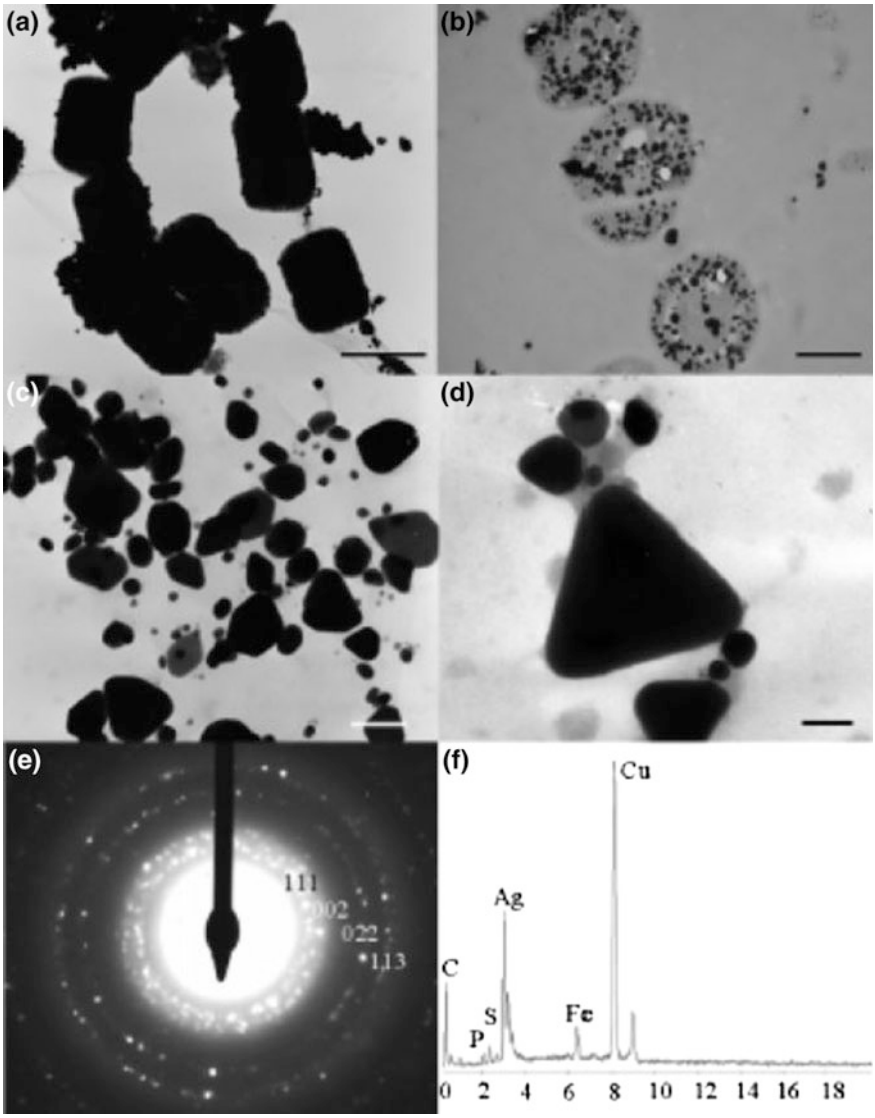


**Fig. 1.8** TEM micrographs of whole mounts of cyanobacterial cells cultured in the presence of $AgNO_3$ at 100 °C and 28 days. **a** Silver nanoparticles encrusted on cyanobacterial cells. **b** TEM micrograph of a thin section of cyanobacteria cells with nanoparticles of silver deposited inside the cell. **c** Octahedral, spherical, and anhedral nanoparticles of silver precipitated in solution. **d** Octahedral silver platelets. **e** TEM-SAED diffraction powder-ring pattern consistent with crystalline nanoparticles of Ag; *d* spacings of 0.235, 0.204, 0.144, and 0.123 nm correspond to reflections 111, 200, 220, and 311, respectively. **f** TEM-EDS for area B. Scale bars in A, B, C, and D are 1, 0.05, and 0.1 and 50 nm, respectively. *Source* Lengke et al. (2007). Copyright © 2007, American Chemical Society. Reproduced with permission

the plasmon absorbance of AgNPs. The crystalline AgNPs were well dispersed in the range of 5–25 nm. Remarkably, the nanoparticles present in the aqueous medium were quite stable, even up to 4 months of incubation at 25 °C. Mukherjee et al. (2008) demonstrated green synthesis of highly stabilized nanocrystalline silver particles by a nonpathogenic and agriculturally important fungus, *Trichoderma asperellum*. An interesting aspect of this study is the mechanism of formation of AgNPs. The process of growing nanoparticles comprises two key steps: bioreduction of $AgNO_3$ to produce AgNPs followed by stabilization and/or encapsulation of the same by a suitable capping agent. The size of the silver particles using TEM and XRD studies is found to be in the range 13–18 nm. These nanoparticles are found to be highly stable and even after prolonged storage for over 6 months they do not show significant aggregation (Fig. 1.9).

A mechanism behind the formation of silver nanoparticles and their stabilization via capping has been investigated using FTIR (Fig. 1.8) and surface-enhanced resonance Raman spectroscopy (Fig. 1.9). Both the spectra exhibit a broad intense band at $\sim$3400 $cm^{-1}$ with overlapping shoulders on either side assigned to the N–H stretching frequency arising from the peptide linkages present in the proteins

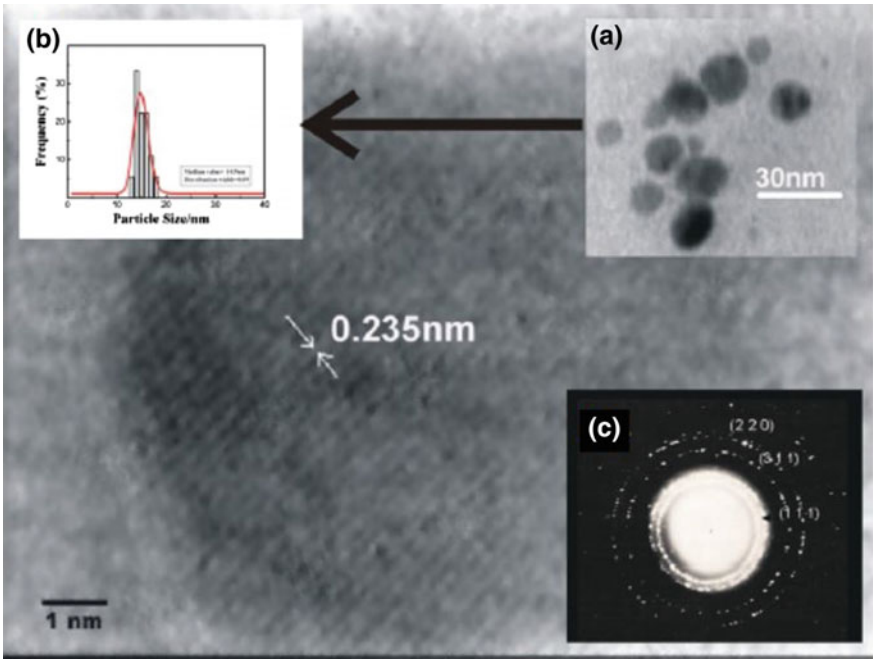


**Fig. 1.9** High-resolution transmission electron micrograph of drop-cast silver nanoparticles preserved for over 6 months. Inset: **a** low-resolution micrographs showing size of the particulates, **b** histogram of particle size distribution as obtained from TEM and **c** SAED pattern recorded on the same sample. *Source* Mukherjee et al. (2008). Copyright © 2008, IOP Science. Reproduced with permission

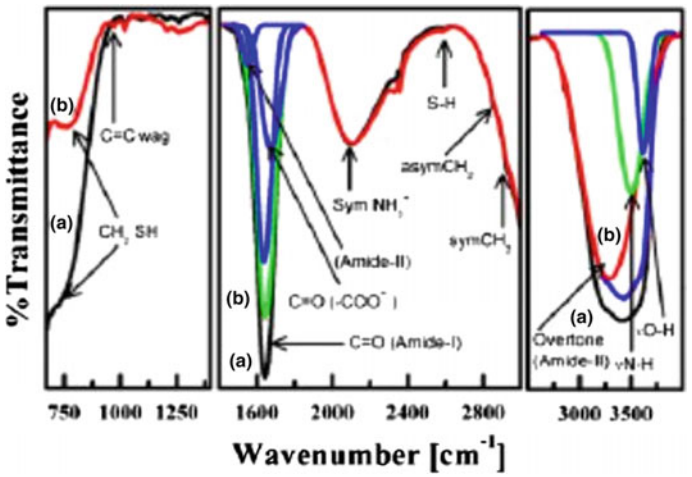


**Fig. 1.10** FTIR spectra of the cell-free extract **a** before addition of $AgNO_3$ and **b** after removal of silver nanoparticles by centrifugation. *Source* Mukherjee et al. (2008). Copyright © 2008, IOP Science. Reproduced with permission

of the extract (Fig. 1.10). Upon deconvolution, the side bands were respectively identified to be the overtone of the amide-II band ($\sim$3270 cm$^{-1}$) and the stretching frequency of the O–H band ($\sim$3600 cm$^{-1}$) possibly arising from the carbohydrates and/or proteins present in the sample. However, it can arise from the aqueous solvent as well. It may be observed that the intensity of the first two bands diminishes significantly in (b), indicating a decrease in the concentration of the peptide linkages in the solution. The spectra also exhibit an intense band at $\sim$1640 cm$^{-1}$ and a broad asymmetric band at $\sim$2100 cm$^{-1}$, the latter assigned to the N–H stretching band in the free amino groups of biomacromolecules and a low intensity peak at $\sim$2600 cm$^{-1}$ due to S–H stretching vibrations. It may be noted that the intensity of the band at $\sim$2100 cm$^{-1}$ remains almost unchanged in the two spectra while that due to S–H stretching shifts towards lower wavenumbers in (b). Upon deconvolution, the band at $\sim$1640 cm$^{-1}$ is found to be a superposition of three different bands centred at $\sim$1550, 1640 and 1670 cm$^{-1}$, respectively assigned to the amide-II band, carbonyl and carboxylic C=O stretching bands of the peptide linkages (Mukherjee et al. 2008).

Figure 1.11 shows the aforesaid Raman spectrum which clearly exhibits an intense band at $\sim$240 cm$^{-1}$ identified to be due to stretching vibrations of Ag–N bonds and two broad bands at $\sim$1350 and 1565 cm$^{-1}$ attributed, respectively, to symmetric and asymmetric C=O stretching vibrations of the $CO_2$ ions apart from a few weak features at $\sim$692, 940, 970 and 1050 cm$^{-1}$ assigned, respectively, to the stretching vibrations of C–S, C–$CO_2$, C–C and Cα–N bonds. Selective enhancement of these Raman bands clearly indicates that C=O bonds of the carboxylate

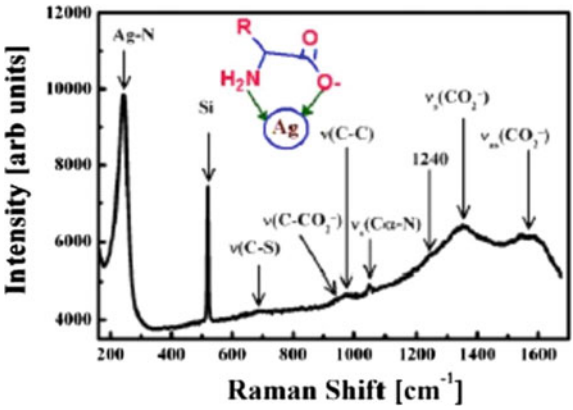


**Fig. 1.11** Macro-Raman spectrum of silver nanoparticles drop-cast on Si (100) single crystals. *Source* Mukherjee et al. (2008). Copyright © 2008, IOP Science. Reproduced with permission

ions and Ag–N bonds from the free amine groups are lying perpendicular to the nano silver surface and are directly associated with the capping of the same. This is further supported from the fact that both the symmetric and asymmetric stretching bands of $CO_2$ are significantly broadened due to distortion in the respective bond angles and bond lengths that have resulted from the strain induced following encapsulation of silver nanoparticles (Mukherjee et al. 2008). The band at 240 $cm^{-1}$ is direct evidence of the formation of a chemical bond between silver nanoparticles and the nitrogen of the amine group present in the amino acids. The probing technique itself manifests the feasibility of using these nanoparticles as potential templates for surface-enhanced resonance Raman spectroscopy (SERS) (Mukherjee et al. 2008). Some other silver nanoparticles produced by microorganisms are listed in Table 1.1.

### *1.2.3 Cadmium Nanoparticles*

The health risks posed by cadmium toxicity have been investigated for over 50 years. Yet knowledge in this area is still expanding, as evidenced by the excellent reviews appearing in this volume. At the level of the organism, cadmium toxicity is associated with liver and kidney injury, osteomalacia, osteoporosis, skeletal deformations, neurological, and other deficits. Cadmium is classified as a category 1 carcinogen, but is not directly genotoxic or mutagenic in bacteria. It is known to affect genome stability via inhibition of DNA repair and generation of free radical-induced DNA damage. At the cellular level, cadmium induces oxidative stress by depletion of endogenous antioxidants such as glutathione and is associated with mitochondrial damage, induction of apoptosis, and disruption of intracellular calcium signaling. Despite the extensive studies on cadmium toxicity, there

continues to be much territory left to cover regarding its mechanism of action, intracellular damage, and environmental exposure. At present, the primary cadmium nanoparticles are those of CdSe or CdTe, encapsulated in various coatings in the form of semiconductor quantum dots (Bao et al. 2010). Semiconductor nano-crystals, which have unique optical, electronic, and optoelectronic properties have potential application in the field of nano-electronics.

Kumar et al. (2007) synthesized CdSe nanoparticles (9–15 nm) using a fungus, *Fusarium oxysporum*, in a mixture of $CdCl_2$ and $SeCl_4$. Cui et al. (2009) synthesized CdSe using a yeast strain: *Saccharomyces cerevisiae*. Pearce et al. (2008) also synthesized CdSe nanoparticles by adding $CdCl_2O_8$ to selenide (Se[II]) produced from selenite (Se[IV]) by an anaerobic bacterium: *Veillonella atypica*. In the latter two studies (Pearce et al. 2008; Cui et al. 2009), cadmium was added after microbial formation of selenide for CdSe synthesis, probably because of its toxicity to the microbes. Consequently, they synthesized CdSe in two-vessel processes consisting of reduction of selenite to selenide and subsequent synthesis of CdSe from selenide and cadmium ion. In contrast, only Kumar et al. (2007) reported a one-vessel process in which the fungus generates CdSe in the co-presence of selenite and cadmium ion, which might improve economic efficiency through its simple operation of fewer reaction vessels. Synthesis of CdSe was observed in *Pseudomonas* sp. RB. by Ayano et al. (2014). Transmission electron microscopy and EDS revealed that this strain accumulated nanoparticles (10–20 nm) consisting of selenium and cadmium inside and on the cells when cultivated in the same medium for the enrichment culture. This report is the first report describing isolation of a selenite-reducing and cadmium-resistant bacterium (Ayano et al. 2014).

Cadmium telluride (CdTe), an important group II–VI semiconductor material with large exciton Bohr radius (7.3 nm) and narrow bulk band gap of 1.5 eV has shown significant potential for LED (energy), FRET (electronics), and biomedical applications (Yang et al. 2009) due to their size dependent properties. These nanoparticles provide excellent photostability, narrow emission and high quantum yield in comparison with organic dyes and therefore explored in live cell bio-imaging (Pan and Feng 2009). Syed and Ahmad (2013) uses the fungus *Fusarium oxysporum* to synthesize highly fluorescent extracellular CdTe (quantum dot) nanoparticles. The process utilizes Cd and Te precursors in a very dilute form and allows bottom-up, one-step preparation of nanoparticles. Different techniques were employed for their characterization such as SAED and XRD which confirmed the crystalline nature of biosynthesized nanoparticles. These biosynthesized nanoparticles are capped by proteins secreted by the fungus in the reaction mixture, which makes them water dispersible and provides stability in solution by preventing their agglomeration. These nanoparticles also showed antibacterial activity against Gram-positive and Gram-negative bacteria. This study demonstrates that fungus based approach provides a novel, rational and environment friendly synthesis protocol for nanomaterials synthesis. This is the first demonstration of a fungal-mediated approach for the synthesis of CdTe quantom dots (Syed and Ahmad 2013).

## 1.3 Alloy Nanoparticles

Alloy nanoparticles or bimetallic nanoparticles exhibit unique electronic, optical, and catalytic properties that are different from those of the corresponding individual metal particles (Harada et al. 1993). For instance gold nanoparticles supported on metal oxide or gold-containing bimetallic nanoparticles are found to exhibit enhanced catalytic activity (Bond 2002).

### *1.3.1 Gold—Silver (Au–Ag) Nanoparticles*

In many functional properties, the performances of Au–Ag alloy nanoparticles are superior to the corresponding monometallic ones, such as in surface enhanced Raman spectroscopy (SERS), sensors, and catalysis. Therefore, many synthesis approaches of bimetallic Au–Ag nanoparticles have been developed, such as digestive ripening, laser synthesis method, seed growth method, ligand binding method, and galvanic reaction. Since the seminal discovery of catalytic activity by gold nanoparticles, supported Au–Ag alloy nanoparticles have been receiving increasing attentions for possible enhancement in catalytic activity (Liu et al. 2013).

In 2005, Liu et al. reported that Au and Ag showed obvious synergetic effect in CO oxidation reaction over an alloy nanocatalyst Au–Ag@MCM-41 catalyst. Since then, the Au–Ag alloy system has been applied to various reactions including oxidation of alcohols, acetylene hydrogenation, and photocatalytic reaction. Sandoval et al. (2011) investigated the Au–Ag alloy nanoparticles supported on $TiO_2$ by a sequential precipitation-deposition method, where they deposited Ag first and Au at the second step, and found that Au–Ag alloy nanoparticles are also very stable under high temperature pretreatment. However, the effect of the deposition sequence on the formation of Au–Ag bimetallic nanoparticles supported on $SiO_2$ and their catalytic performances have not been investigated yet. Since Sun and Xia (2002) found the replacement reaction method could synthesize Au–Ag bimetallic systems, various Au–Ag nanostructures have been developed including hollow cubes, porous surfaces and alloy nanoparticles.

Senapati et al. (2005) reported the synthesis of bimetallic Au–Ag alloy by *Fusarium oxysporum* and argued that the secreted cofactor NADH plays an important role in determining the composition of Au–Ag alloy nanoparticles. Using TEM, well-separated nanoparticles with occasional aggregation in the size range 8–14 nm are clearly observed (Fig. 1.12). The amount of cofactor NADH plays an important role in determining the nanoalloy composition (Senapati et al. 2005).

Zheng et al. (2010) studied Au–Ag alloy nanoparticles biosynthesized by yeast cells (Fig. 1.13). Fluorescence microscopic and transmission electron microscopic characterizations indicated that the Au–Ag alloy nanoparticles were mainly synthesized via an extracellular approach and generally existed in the form of irregular

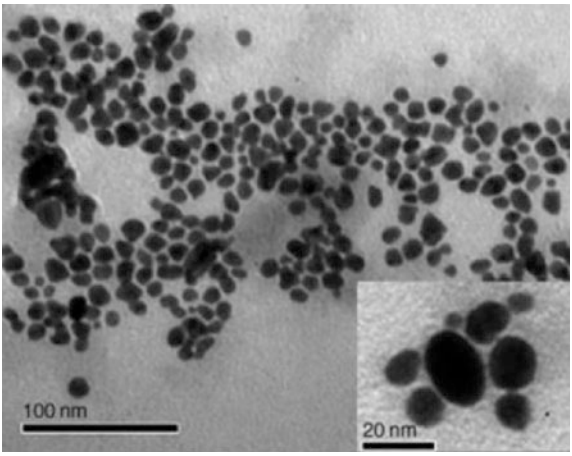


**Fig. 1.12** TEM images of Au–Ag nanoparticles formed by reaction of a mixture of 1 mm $HAuCl_4$ and 1 mm $AgNO_3$ with 60 g *Fusarium oxysporum* wet biomass for 96 h. *Source* Senapati et al. (2005). Copyright © 2013, Wiley-VCH Verlag GmbH & Co. KGaA. Reproduced with permission

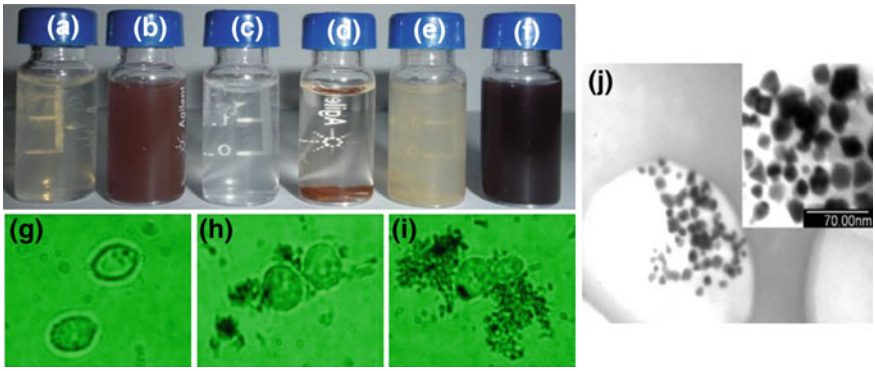


**Fig. 1.13** Yeast cell solutions containing $HAuCl_4$ (**a** and **b**), $AgNO_3$ (**c** and **d**) and the mixture of $HAuCl_4$ and $AgNO_3$ (**e** and **f**) before (**a**, **c** and **e**) and after (**b**, **d** and **f**) standing for 24 h, fluorescence microscopy bright field images of the surface of yeast cells' film after reacting with $AgNO_3$ (**g**), $HAuCl_4$ (**h**) and the mixture of $AgNO_3$ and $HAuCl_4$ (**i**), and TEM images of Au–Ag alloy nanoparticles (**j**). *Source* Zheng et al. (2010). Copyright © 2010, Elsevier. Reproduced with permission

polygonal nanoparticles. Electrochemical investigations revealed that the vanillin sensor based on Au–Ag alloy nanoparticles modified glassy carbon electrode was able to enhance the electrochemical response of vanillin for at least five times.

Sawle et al. (2008) demonstrated the synthesis of core-shell Au–Ag alloy nanoparticles from fungal strains *Fusarium semitectum* and showed that the

nanoparticle suspensions are quite stable for many weeks. As *Fusarium. oxysporum* is known to synthesize technologically important metal sulfide quantum dots extracellularly, this procedure can further be extended for the synthesis of other composite nanoparticles such as Au–CdS, Ag–CdS, and CdS–PbS.

## 1.4 Oxide Nanoparticles

The industrial use of metallic oxide nanoparticles in a wide variety of applications has been rapidly expanding in the last decade. Such applications include the use of silicon, titanium, iron, and other metallic oxide nanoparticles, thereby increasing the occupational and other environmental exposure of these nanoparticles to humans and other species (Lai et al. 2007a). Nevertheless, the health effects of exposure of humans and other species to metallic oxide nanoparticles have not been systematically investigated as their impact on the environment has not been under the scrutiny of regulatory control (Lai et al. 2007b). Oxide nanoparticle is an important type of compound nanoparticle synthesized by microbes. In this section, Li et al. (2011) reviewed the biosynthesis of oxide nanoparticles. Most of the examples of the magnetotactic bacteria used for the production of magnetic oxide nanoparticles and biological systems for the formation of nonmagnetic oxide nanoparticles (Table 1.2).

### *1.4.1 Cerium Oxide Nanoparticles*

Cerium, which is the first element in the lanthanide group with 4*f* electrons, has attracted much attention from researchers in physics, chemistry, biology and materials science. It is the most abundant of rare-earth metals found in the Earth's crust. Several Ce-carbonate, -phosphate, -silicate, and -(hydr)oxide minerals have been historically mined and processed for pharmaceutical uses and industrial applications. Of all Ce minerals, cerium dioxide has received much attention in the global nanotechnology market due to their useful applications for catalysts, fuel cells, and fuel additives. When combined with oxygen in a nanoparticle formulation, cerium oxide adopts a fluorite crystalline structure that emerges as a fascinating material. This cerium oxide nanoparticle (CeONP) has been used prolifically in various engineering and biological applications, such as solid-oxide fuel cells, high-temperature oxidation protection materials, catalytic materials,, solar cells and potential pharmacological agents (Xu and Qu 2014). Although useful because of its various properties and applications, the main application of CeONPs is in the field of catalysis, and stems from their unique structure and atomic properties compared with other materials. Cerium nanoparticles have found numerous applications in the biomedical industry due to their strong antioxidant properties. Industrial applications include its use as a polishing agent, ultraviolet absorbing compound in

**Table 1.2** Oxide nanoparticles synthesized by microorganisms

| Microorganism | Type nanoparticle produce | Size (nm) | Shape | Reference |
|---|---|---|---|---|
| *Curvularia lunata* | $CeO_2$ | 5 | Spherical | Munusamy et al. (2016) |
| *Fusarium oxysporum* | $TiO_2$ | 6–13 | Spherical | Bansal et al. (2005) |
| *Fusarium oxysporum* | $BaTiO_3$ | 4–5 | Spherical | Bansal et al. (2006) |
| *Fusarium oxysporum* | $ZrO_2$ | 3–11 | Spherical | Bansal et al. (2004) |
| *Lactobacillus* sp. | $BaTiO_3$ | 20–80 | Tetragonal | Jha and Prasad (2010) |
| *Lactobacillus* sp. | $T1O_2$ | 8–35 | Spherical | Jha et al. (2009a) |
| *Saccharomyces cerevisiae* | $Sb_2O_3$ | 2–10 | Spherical | Jha et al. (2009b) |
| *Shewanella oneidensis* | $Fe_3O_4$ | 40–50 | Rectangular, rhombic, hexagonal | Perez-Gonzalez et al. (2010) |
| *Shewanella oneidensis* MR-1 | $Fe_3O_3$ | 30–43 | Pseudohexagonal/irregular or rhombohedral | Bose et al. (2009) |
| *Yeast cells* | $Fe_3O_4$ | Not available | Wormhole- like | Zhou et al. (2009) |
| *Penicillium* sp. | CuO | Not available | Spherical | Honary et al. (2012) |
| *Fusarium oxysporum* | CuO | 2–5 | Spherical | Hosseini et al. (2012) |
| *Stereum hirsutum* | CuO | 5–20 | Spherical | Cuevas et al. (2015) |

sunscreen, solid electrolytes in solid oxide fuel cells, as a fuel additive to promote combustion, and in automotive exhaust catalysts (Sindhu et al. 2015). CeONPs have also been used in fighting inflammation and cancer, and in radiation protection of cells (Shah et al. 2012).

A recent mass flow modeling study predicted that a major source of $CeO_2$ nanoparticles from industrial processing plants (e.g., electronics and optics manufactures) is likely to reach the terrestrial environment such as landfills and soils. The environmental fate of $CeO_2$ nanoparticles is highly dependent on its physicochemical properties in low temperature geochemical environment. Though there are needs in improving the analytical method in detecting/quantifying $CeO_2$ nanoparticles in different environmental media, it is clear that aquatic and terrestrial organisms have been exposed to $CeO_2$ NPs, potentially yielding in negative impact on human and ecosystem health. Interestingly, there has been contradicting reports about the toxicological effects of $CeO_2$ nanoparticles, acting as either an antioxidant

or reactive oxygen species production-inducing agent) (Dahle and Arai 2015). This poses a challenge in future regulations for the $CeO_2$ nanoparticle application and the risk assessment in the environment.

Arumugam et al. (2015) successfully synthesize $CeO_2$ nanoparticles using *Gloriosa superba* L. leaf extract. The synthesized nanoparticles retained the cubic structure, which was confirmed by X-ray diffraction studies. The oxidation states of the elements (C [1s], O [1s] and Ce [3d]) were confirmed by XPS studies. TEM images showed that the $CeO_2$ nanoparticles possessed spherical shape and particle size of 5 nm. The Ce–O stretching bands were observed at 451 $cm^{-1}$ and 457 $cm^{-1}$ from the FT-IR and Raman spectra respectively. The band gap of the $CeO_2$ NPs was estimated as 3.78 eV from the UV–visible spectrum. From the photoluminescence measurements, the broad emission composed of eight different bands were found. The antibacterial studies performed against a set of bacterial strains showed that Gram-positive bacteria were relatively more susceptible to the NPs than Gram-negative bacteria. The toxicological behavior of $CeO_2$ NPs was found due to the synthesized NPs with uneven ridges and oxygen defects in $CeO_2$ NPs.

$CeO_2$ NPs have been successfully synthesized using the fungus *Curvularia lunata* (Munusamy et al. 2016). The XRD patterns, Micro Raman spectra and SAED pattern studies suggest the formation $CeO_2$ NPs cubic fluorite structure. The TEM images showed spherical morphology with the average size of 5 nm. Synthesized $CeO_2$ NPs were investigated by antibacterial activity. The perusal results observed at 100 μg $CeO_2$ NPs had most significant effect of antibacterial activity due to the strong electrostatic forces to binding the bacterial cell membrane to inhibit the bacterial growth.

### *1.4.2 Silica Dioxide Nanoparticles*

Silica, or silicon dioxide, is the same material used to make glass. In nature, silica makes up quartz and the sand you walk on at the beach. Unlike metals such as gold and iron, silica is a poor conductor of both electrons and heat. Despite these limitations, silica (silicon oxide) nanoparticles form the framework of silica aerogels. *Silica aerogels* are composed of silica nanoparticles interspersed with nanopores filled with air. As a result, this substance is mostly made up of air. Because air has very low thermal conductivity and silica has low thermal conductivity, they are great materials to use in insulators. These properties make nano aerogels one of the best thermal insulators known to man. Silica nanoparticles can also be functionalized by bonding molecules to a nanoparticle that also is able to bond to another surface, such as a cotton fiber. The functionalized silica nanoparticles attach to the cotton fiber and form a rough surface that is hydrophobic (water repellent), giving an effect similar to the water repellency of lotus leaves. Another type of silica nanoparticle is riddled with nanoscale pores. Researchers are developing drug delivery methods where therapeutic molecules stored inside the pores are slowly released in a diseased region of the body, such as near a cancer tumor (Argyo et al. 2014).

Application of silica nanoparticles as fillers in the preparation of nanocomposite of polymers has drawn much attention, due to the increased demand for new materials with improved thermal, mechanical, physical, and chemical properties. The chemical synthesis of silica-based materials are relatively expensive and exo-hazardous, often requiring extreme temperature, pressure and pH. Singh et al. (2008) demonstrated the synthesis of silicon/silica nanoparticle composites by *Acinetobacter* sp. The formation of silicon/silica nanocomposite is shown to occur when the bacterium is exposed to $K_2SiF_6$ precursor under ambient conditions. This bacterium has been shown to synthesize iron oxide and iron sulfide nanoparticles. It is hypothesized that this bacterium secretes reductases and oxidizing enzymes which lead to $Si/SiO_2$ nanocomposite synthesis. The synthesis of silica nanoparticles by bacteria demonstrates the versatility of the organism, and the formation of elemental silicon by this environmentally friendly process expands further the scope of microorganism-based nanomaterial synthesis.

### *1.4.3 Titatium Oxide Nanoparticles*

Titanium dioxide ($TiO_2$) has become part of our everyday lives. It is found in various consumer goods and products of daily use such as cosmetics, paints, dyes and varnishes, textiles, paper and plastics, food and drugs, and even paving stones. 4.68 million tons of titanium dioxide were produced worldwide in 2009. Titanium dioxide ($TiO_2$) is a material of great significance in many fields, e.g., photocatalysis, solar cell devices, gas sensors, and biomaterials (Gong and Selloni 2005). The non-toxic and biocompatible properties of Titania find its applications in biomedical sciences such as bone tissue engineering as well as in pharmaceutical industries (Jha et al. 2009a). $TiO_2$ catalysts have been confirmed to be excellent and efficient photocatalysts for the degradation and inhibition of numerous toxic environmental contaminants. Various applications of titanium dioxide include air and water cleaning and surface cleaning (Pan et al. 2010). Titanium is recommended for desalinization plants because of its strong resistance to corrosion from seawater. In medical applications the titanium pins are due to because of their non-reactive nature when contacting bone and flesh (Prasad et al. 2007). The $TiO_2$ nanoparticles are synthesized using various methods such as sol gel, hydrothermal, flame combustion, solvothermal, fungal mediated biosynthesis

Titanium oxide nanoparticles can be synthesized from *Bacillus subtilis* (Kirthi et al. 2011). The $TiO_2$ nanoparticles have shown spherical clusters of the nanoparticles. Nanoparticles were spherical, oval in shape, individual as well as a few aggregates having the size of 66–77 nm. The particle size distribution reveals the morphological homogeneity with the grain size falling mostly in submicron range. The energy yielding material—glucose, which controls the value of oxidation—reduction potential ($rH_2$), the ionic status of the medium pH and overall $rH_2$, which is partially controlled by the bicarbonate, negotiate the synthesis of $TiO_2$ nanoparticles in the presence of *B. subtilis*. The synthesis of n-$TiO_2$ might have

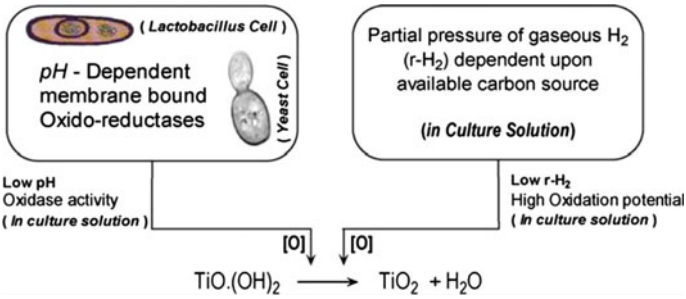


**Fig. 1.14** Schematics for the biosynthesis of *n*-$TiO_2$. *Source* Jha et al. (2009a). Copyright © 2009, Elsevier. Reproduced with permission

resulted due to pH-sensitive membrane bound oxidoreductases and carbon source dependent $rH_2$ in the culture solution (Kirthi et al. 2011).

A low-cost green and reproducible microbes (*Lactobacillus* sp. and *Saccharomyces cerevisiae*) mediated biosynthesis of $TiO_2$ nanoparticles was carried out by Jha et al. (2009a). The synthesis was performed akin to room temperature in the laboratory ambience. X-ray and transmission electron microscopy analyses were performed to ascertain the formation of $TiO_2$ nanoparticles. Individual nanoparticles as well as a few aggregate having the size of 8–35 nm are found. Concentric Scherrer rings in the selected area electron diffraction pattern indicated that the nanoparticles are having all possible orientations. A possible involved mechanism for the biosynthesis of nano-$TiO_2$ has also been proposed in which pH as well as partial pressure of gaseous hydrogen ($rH_2$) or redox potential of the culture solution seems to play an important role in the process (Fig. 1.14).

### *1.4.4 Iron Oxide Nanoparticles*

Eight iron oxides are known (Cornell and Schwertmann 2003), among these iron oxides, hematite (α-$Fe_2O_3$), magnetite ($Fe_3O_4$) and maghemite (γ-$Fe_2O_3$) are very promising and popular candidates due to their polymorphism involving temperature-induced phase transition. Each of these three iron oxides has unique biochemical, magnetic, catalytic, and other properties which provide suitability for specific technical and biomedical applications. As the most stable iron oxide and n-type semiconductor under ambient conditions, hematite (α-$Fe_2O_3$) is widely used in catalysts, pigments and gas sensors due to its low cost and high resistance to corrosion. It can also be used as a starting material for the synthesis of magnetite ($Fe_3O_4$) and maghemite (γ-$Fe_2O_3$), which have been intensively pursued for both fundamental scientific interests and technological applications in the last few decades (Wu et al. 2010a). As shown in Fig. 1.15b, $Fe_3O_4$ has the face centered cubic spinel structure, based on 32 $O_2^-$ ions and close-packed along the direction. $Fe_3O_4$ differs from most

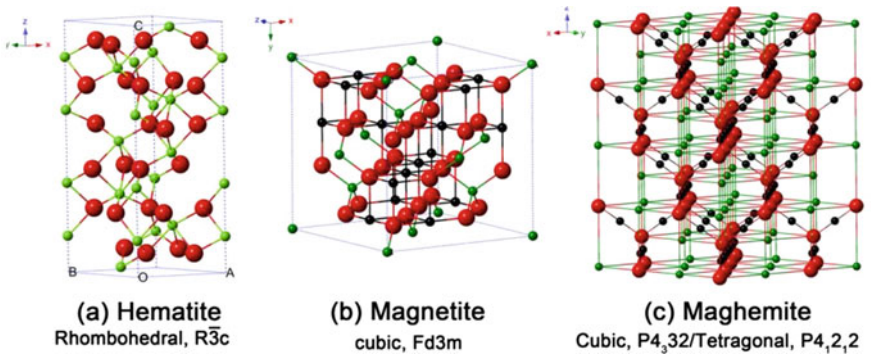


**Fig. 1.15** Crystal structure and crystallographic data of the hematite, magnetite and maghemite (the *black ball* is $Fe^{2+}$, the *green ball* is $Fe^{3+}$ and the *red ball* is $O_2$. *Source* Wu et al. (2015). Copyright © 2015, Taylor and Francis. Reproduced with permission

other iron oxides in that it contains both divalent and trivalent iron. $Fe_3O_4$ has a cubic inverse spinel structure that consists of a cubic close packed array of oxide ions, where all of the $Fe^{2+}$ ions occupy half of the octahedral sites and the $Fe^{3+}$ are split evenly across the remaining octahedral sites and the tetrahedral sites. $Fe_3O_4$ has the lowest resistivity among iron oxides due to its small bandgap (0.1 eV). As shown in Fig. 1.15c, the structure of γ-$Fe_2O_3$ is cubic; each unit of maghemite contains 32 $O_2^-$ ions, 211/3 $Fe^{3+}$ ions and 21/3 vacancies. Oxygen anions give rise to a cubic close-packed array while ferric ions are distributed over tetrahedral sites (eight Fe ions per unit cell) and octahedral sites (the remaining Fe ions and vacancies). Therefore, the maghemite can be considered as fully oxidized magnetite, and it is an n-type semiconductor with a bandgap of 2.0 eV.

The bacterium *Actinobacter* sp. has been shown to be capable of extracellularly synthesizing iron based magnetic nanoparticles, namely maghemite (γ-$Fe_2O_3$) and greigite ($Fe_3S_4$) under ambient conditions depending on the nature of precursors used (Bharde et al. 2008). More precisely, the bacterium synthesized maghemite when reacted with ferric chloride and iron sulfide when exposed to the aqueous solution of ferric chloride-ferrous sulfate. Challenging the bacterium with different metal ions resulted in induction of different proteins, which bring about the specific biochemical transformations in each case leading to the observed products. Maghemite and iron sulfide nanoparticles show superparamagnetic characteristics as expected. Compared to the earlier reports of magnetite and greigite synthesis by magnetotactic bacteria and iron reducing bacteria, which take place strictly under anaerobic conditions, the present procedure offers significant advancement since the reaction occurs under aerobic condition. Moreover, reaction end products can be tuned by the choice of precursors used. The process of magnetic nanoparticles mineralization can be divided into four steps (Faramazi and Sadighi 2013): (1) vesicle formation and iron transport from outside of the bacterial membrane into the cell; (2) magnetosomes alignment in chain; (3) initiation of crystallization; and (4) crystal maturation (Fig. 1.16).

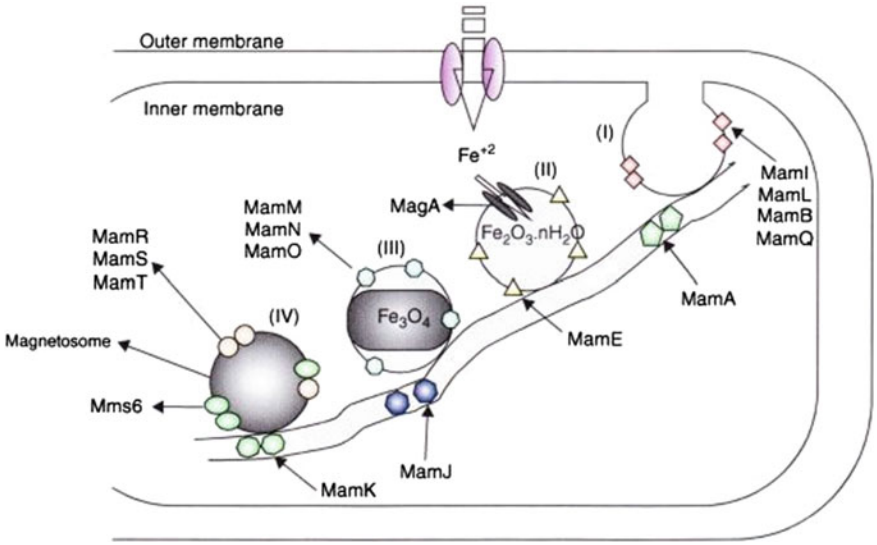


**Fig. 1.16** Magnetosome biomineralization in magnetotactic bacteria (MTB). (*I*) MamI, MamL, MamB, and MamQ proteins initiate the membrane invagination and form a vesicular membrane around the magnetosome structure. (*II*) The protease-independent function of MamE recruits other proteins such as MamK, MamJ and MamA to align magnetosomes in a chaib. (*III*) Iron uptake occurs via MagA, a transmembrane protein, and initiation of magnetic crystal biomineralization occurs through MamM, MamNm and MamO proteins. (*IV*) Finally, MamR, MamS, MamT, MamP, MamC, MamD, MamF, MamG, the protease-dependent of MamE and Mms6, a membrane tightly bounded GTPase, regulate crystal growth and determine morphology of the produced magnetic nanoparticles. *Source* Faramazi and Sadighi (2013). Copyright © 2013, Elsevier. Reproduced with permission

### *1.4.5 Zirconium Dioxide ($ZrO_2$) Nanoparticles*

Zirconium is a strong transition metal that resembles titanium. Because of its strong resistance to corrosion, it is used as an alloying agent in materials that are exposed to corrosive agents such as surgical appliances, explosive primers, vacuum tube getters and filaments. Since it has a very negative reduction potential (−1.55 V), it is never found as the native metal. It is obtained mainly from the mineral zircon, which can be purified with chlorine (Eshed et al. 2011). Because of its intrinsic physicochemical properties such as hardness, shock wear, strong acid and alkali resistance, low frictional resistance, and high melting temperature, zirconia can be used as an abrasive, as a hard, resistant coating for cutting tools, and in high temperature engine components. For these reasons, it is often called ceramic steel. Zirconia nanoparticles are of great interest due to their improved optical and electronic properties with application as a piezoelectric, electro-optic and dielectric material. Zirconia is also emerging as an important class of catalyst. The synthesis of zirconia has been realized by physico-chemical methods such as sol–gel synthesis, aqueous precipitation,

thermal decomposition and hydrothermal synthesis (Bansal et al. 2004). However, all these methods require extremes of temperature (in the case of thermal synthesis) and pressure (hydrothermal synthesis).

Bansal et al. (2004) have shown that the fungus *Fusarium oxysporum* secretes proteins capable of hydrolyzing aqueous $ZrF_6^{2-}$ ions extracellularly to form zirconia at room temperature. Particularly interesting is the fact that the fungus is capable of hydrolyzing tough metal halide precursors under acidic conditions. While the hydrolytic proteins secreted by *Fusarium oxysporum* are yet to be sequenced and studied for their role in the fungus metabolic pathways, our studies indicate that they are cationic proteins of molecular weight centered around 24 and 28 kDa and thus, similar to silicatein. The regenerative capability of biological systems coupled with the fact that that fungi such as *Fusarium oxysporu*m are capable of hydrolyzing metal complexes that they never encounter during their growth cycle shows enormous promise for development, particularly in large-scale synthesis of metal oxides.

### 1.4.6 Antimony Trioxide ($Sb_2O_3$) Nanoparticles

Antimony trioxide ($Sb_2O_3$) is a good semiconducting material and an excellent catalyst for the production of PET plastic used in the packaging of mineral water and soft drinks, which has been confirmed by the World Health Organization and the European Food Safety Authority. In addition, $Sb_2O_3$/$Sb_2O_5$ is a potential compound for the synthesis of antimony gluconate, which is considered to be an effective medicine against Kala azar (visceral leishmaniasis). Common salts of antimony are irritants, thus an oral administration produces nausea, vomiting and diarrhea; they are therefore administered parenterally. It is also a cumulative drug. Antimony compounds are avoided in cases of pulmonary tuberculosis, jaundice, nephrites and dysentery (Acharya 1972). Nanoscale antimony compounds could prove to be less toxic to the body because they can cross the renal barrier. Further, $Sb_2O_3$ greatly increases flame retardant effectiveness when used as a synergist in combination with halogenated flame retardants in plastics, paints, adhesives, sealants, rubber and textile back coatings (Ye et al. 2006). $Sb_2O_3$ also has several applications, such as a fining agent or as a degasser (to remove bubbles) in glass manufacturing, an opacifier in porcelain and enameling services, and a white pigment in paints. $Sb_2O_3$ nanoparticles have been synthesized using different techniques by different groups of researchers (Guo et al. 2000; Friedrichs et al. 2001; Ye et al. 2002). A microbe (*Lactobacillus* sp.)-mediated biosynthesis of $Sb_2O_3$ nanoparticles was reported by Jha et al. (2009b). The synthesis was performed at around room temperature. X-ray and transmission electron microscopy analyses were performed to ascertain the formation of $Sb_2O_3$ nanoparticles. X-ray analysis indicated that $Sb_2O_3$ nanoparticles had a face-centered cubic unit cell structure. Individual nanoparticles as well as a few aggregate of 3–12 nm were found.

### 1.4.7 Copper Oxide (CuO) Nanoparticles

Copper as a metal or copper oxides exhibit broad-spectrum biocidal activity, and several studies during the last two years found that copper demonstrates remarkable antibacterial activity at the nanoscale (Cuevas et al. 2015). In contrast to silver nanoparticles, which have been studied extensively for antibacterial application, copper is an essential element for living organisms and may be suitable for biomedical applications (Rubilar et al. 2013). It is important to note that copper is approximately 10-fold cheaper than silver in the market, and therefore, a method utilizing copper would prove to be quite cost-effective. On the other hand, it has been reported that copper nanoparticles are less toxic than silver nanoparticles (Bondarenko et al. 2013). Microorganisms such as *Fusarium oxysporum* are able to leach copper from integrated circuits present on electronic boards under ambient conditions (Cuevas et al. 2015). The analysis of the biogenic synthesis of copper oxides from $CuSO_4$ has been observed in by *Penicillium aurantiogriseum*, *P. citrinum*, *P. waksmanii*, and *F. oxysporum* showed no large polydispersity in the pH range of 5–9 (Honary et al. 2012; Hosseini et al. 2012). A limited number of studies have been published, and these evaluated different fungal strains for the biosynthesis of copper nanoparticles. Fungi, such as *Penicillium* sp. and *F. oxysporum* strains, have been reported to biosynthesize copper oxide and $Cu_2S$ nanoparticles (Honary et al. 2012; Hosseini et al. 2012).

Cuevas et al. (2015) evaluated the ability to synthesize copper and copper oxide nanoparticles using a mycelium-free extract produced by *Stereum hirsutum*, a white-rot fungus, in the presence of three different copper salts and to characterize and assess the involvement of proteins in the formation of the nanoparticles. The nanoparticles biosynthesis in presence of all copper salts demonstrated higher formation with 5 mM $CuCl_2$ under alkaline conditions. TEM analysis confirmed that the nanoparticles were mainly spherical (5–20 nm). The presence of amine groups attached to nanoparticles was confirmed by FTIR, which suggests that extracellular protein of fungus is responsible for the formation of the nanoparticles.

### 1.4.8 Zinc Oxide (ZnO)

Zinc oxide (ZnO) NPs have unique optical and electrical properties, and as a wide band gap semiconductor, they have found more uses in biosensors, nanoelectronics, and solar cells. These NPs are being used in the cosmetic and sunscreen industry due to their transparency and ability to reflect, scatter, and absorb UV radiation and as food additives. Furthermore, zinc oxide NPs are also being considered for use in next-generation biological applications including antimicrobial agents, drug delivery, and bioimaging probes (Jayaseelan et al. 2012). A low-cost and simple procedure for synthesis of zinc oxide NPs using reproducible bacterium, *Aeromonas hydrophila*, was reported. X-ray diffraction (XRD) confirmed the crystalline nature

of the NPs, and atomic force microscopy (AFM) showed the morphology of the nanoparticle to be spherical, oval with an average size of 57.72 nm. The antibacterial and antifungal activity was ended with corresponding well diffusion and minimum inhibitory concentration. The maximum zone of inhibition was observed in the ZnO NPs (25 μg/mL) against *Pseudomonas aeruginosa* ($\sim 22 \pm 1.8$ mm) and *Aspergillus flavus* ($\sim 19 \pm 1.0$ mm) (Jayaseelan et al. 2012).

## 1.5 Sulfide Nanoparticles

In addition to oxide nanoparticles, sulfide nanoparticles have also attracted great attention in both fundamental research and technical applications as quantum-dot fluorescent biomarkers and cell labeling agents because of their interesting and novel electronic and optical properties (Yang et al. 2005). Examples of sulfide-producing nanoparticles are listed in Table 1.3.

**Table 1.3** Sulfide nanoparticles synthesized by microorganisms

| Microorganism | Type nanoparticle produce | Size (nm) | Shape | Reference |
|---|---|---|---|---|
| *Coriolus versicolor* | CdS | 100–200 | Spherical | Sanghi and Verma (2009) |
| *Desulfobacteraceae* | CdS | 2–5 | Hexagonal lattice | Labrenz et al. (2000) |
| *Escherichia coli* | CdS | 2–5 | Wurtzite crystal | Sweeney et al. (2004) |
| *Fusarium oxysporum* | CdS | 5–20 | Spherical | Ahmad et al. (2002) |
| *Lactobacillus* | CdS | 4.7–5.1 | Spherical | Prasad and Jha (2010) |
| *Rhodopseudomonas palustris* | CdS | 8 | Cubic | Bai et al. (2009) |
| *Schizosaccharomyces pombe* | CdS | 1–1.5 | Hexagonal lattice | Kowshik et al. (2002) |
| Yeast | CdS | 3.4–3.8 | Spherical | Prasad and Jha (2010) |
| *Rhodopseudomonas sphaeroides* | PbS | 10.35–10.65 | Spherical | Bai and Zhang (2009) |
| Sulfate-reducing bacteria | FeS | 2 | Spherical | Watson et al. (1999) |
| *Fusarium oxysporum* | CuS | 10–40 | Not available | Schaffie and Hosseini (2014) |
| *Rhodopseudomonas sphaeroides* | ZnS | 8 | Hexagonal lattice | Bai et al. (2006) |

### 1.5.1 Cadmium Sulfide (CdS) Nanoparticles

CdS nanocrystal is one typical type of sulfide nanoparticle and has been synthesized by microorganisms (Prasad and Jha 2010; Kowshik et al. 2002). Cunningham and Lundie found that *Clostridium thermoaceticum* could precipitate CdS on the cell surface as well as in the medium from $CdCl_2$ in the presence of cysteine hydrochloride in the growth medium where cysteine most probably acts as the source of sulfide (Cunningham and Lundie 1993). Dameron et al. (1989) have used *Schizosaccharomyces pombe* and *Candida glabrata* (yeasts) to produce intracellular CdS nanoparticles with cadmium salt solution. ZnS and PbS nanoparticles were successfully synthesized by biological systems. *Rhodobacter sphaeroides* and *Desulfobacteraceae* have been used to obtain ZnS nanoparticles intracellularly with 8 nm and 2–5 nm in average diameter, respectively (Bai et al. 2006; Labrenz et al. 2000).

Kang et al. (2008) reported phytochelatin-mediated intracellular synthesis of CdS nanocrystals in engineered *E. coli*. By controlling the population of the phytochelatin (PCs), *E. coli* cells were engineered as an eco-friendly biofactory to produce uniformly sized PC-coated CdS nano-crystals. This is the first systematic approach toward tunable synthesis of semiconductor nano-crystals by genetically engineered bacteria. The first report on the production of semiconductor nano-crystal synthesis in bacteria was published by Sweeney et al. (2004). The study revealed that *E. coli* has the endogenous ability to direct the growth of nano-crystals. Parameters such as growth phase and strain type are essential for initiating nano-crystal growth. El-Shanshoury et al. (2012) reported a rapid and low-cost biosynthesis of CdS using culture supernatants of *Escherichia coli* ATCC 8739, *Bacillus subtilis* ATCC 6633, and *Lactobacillus acidophilus* DSMZ 20079T. The CdS nanoparticles synthesis were performed at room temperature and were formed within 24 h. The process of extracellular and fast biosynthesis may help in the development of an easy and eco-friendly route for synthesis of CdS nanoparticles. Mousavi et al. (2012) reported the synthesis of CdS nanoparticles using *Escherichia coli* PTTC 1533 and *Klebsiella pneumoniae* PTTC 1053. The synthesis of 5-200 nm nanoparticles occurred after 96 h of incubation at 30 °C and pH 9.

A plausible mechanism has been made to understand the synthesis of CdS nanoparticles (Fig. 1.17). At the initial phase of the reaction, $CdCl_2$ dissociates into $Cd^{2+}$ and accumulates around the bacterial membrane because of the negative potential of the bacterial membrane (Triphati et al. 2014). $Cd^{2+}$ being a heavy metal ion creates stress conditions for bacteria, thus leading bacterial biomass to initiate a defense mechanism. This leads bacteria to secrete certain enzymes/proteins in order to detoxify the metal ions that created the metal stress condition. The secreted protein by bacterial biomass binds up with $Cd^{2+}$. Subsequently, $Na_2S$ being added dissociates into $S^{2-}$ in the solution and it also binds with the protein. The CdS nuclei then grow following the process of Ostwald ripening leading to the formation of CdS nanoparticles. Thus, protein secreted in this process becomes incorporated as it serves a capping layer for synthesis of CdS nanoparticles (Triphati et al. 2014).

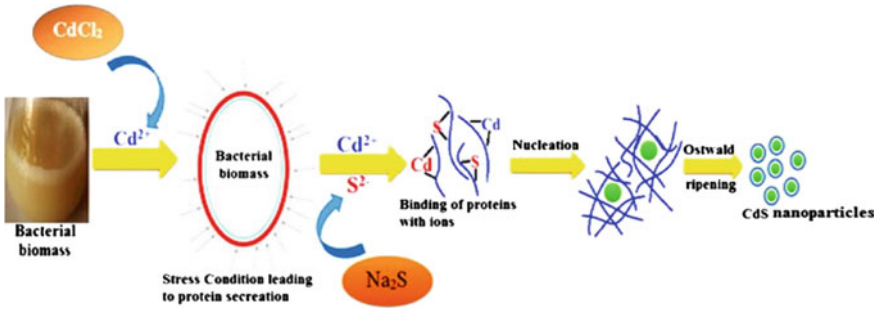


**Fig. 1.17** Biosynthesis mechanism of CdS nanoparticles. *Source* Tripathi et al. (2014). Copyright © 2014, IOP Science

### *1.5.2 Lead Sulfide (PbS) Nanoparticles*

Semiconductor PbS nanoparticles have attracted great attention in recent decades as a result of their interesting optical and electronic properties, and some of them are used for the fabrication of devices size (Bai and Zhang 2009). Some new chemical methods for the preparation of lead sulfide nanoparticles require special container, high temperature or long time for initiating the reaction. Biological synthesis method is one of the promising methods due to requiring a relatively milder condition, one step synthetic procedure, clean, and controllable size distribution. An earlier study found that *Torulopsis* sp. is capable of synthesizing PbS nanocrystals intracellularly when challenged with $Pb^{2+}$. PbS nanoparticles were also synthesized by using *Rhodobacter sphaeroides*, whose diameters were controlled by the culture time (Bai and Zhang 2009).

### *1.5.3 Iron Sulfide Nanoparticles*

Ahmad et al. (2002) have found eukaryotic organisms such as fungi to be a good candidate for the synthesis of metal sulfide nanoparticles extracellularly. Another kind of sulfide nanoparticle was magnetic $Fe_3S_4$ or FeS nanoparticle. Bazylinski et al. (1995) reported the formation of $Fe_3S_4$ by uncultured magnetotactic bacteria. They examined a sediment sample that contained approximately $1 \times 10^5$ magnetotactic bacteria per $cm^3$, and approximately $10^5$ cells were obtained after purification by the racetrack method. Magnetosomes in the uncultured cells exhibited elongated rectangular shape. The average magnetosome number per cell was approximately 40, and they were mainly located as a large cluster within the cell. Aligned magnetosomes forming a chainlike structure were also observed beside the large cluster. Sulfate-reducing bacteria were capable of producing magnetic FeS nanoparticles (Watson et al. 1999).

### 1.5.4 Copper Sulfide Nanoparticles

Copper sulfide (CuS) nanoparticles have attracted increasing attention from biomedical researchers across the globe, because of their intriguing properties which have been mainly explored for energy- and catalysis-related applications to date. Recently, CuS nanoparticles are gradually emerging as a promising platform for sensing, molecular imaging, photothermal therapy, drug delivery, as well as multifunctional agents that can integrate both imaging and therapy (Goel et al. 2014). Although copper sulfide nanoparticles have been previously synthesized by several chemical, electrochemical, organic and enzymatic methods, the first report on a biosynthesis approach was published in 2012 by Hosseini et al. in which the copper sulfide nanoparticles were synthesized from a pure copper sulfate solution by *F. oxysporum*. Industrially, the heavy metals in wastewaters are precipitated in the sulfide forms via dissimilatory reduction of sulfate that is performed by anaerobes. However, the performance of these sulfate-reducing bacteria is limited to anaerobic environments. Metal sulfides are also formed from sulfate by assimilatory sulfate reduction (Tiquia 2008; Tiquia et al. 2006) performed via aerobic pathways by overproducing two unique enzymes called serine acetyltransferase (SAT) and cysteine desulfhydrase. The precursor of cysteine biosynthesis (O-acetylserine) is produced by the acetylation of serine that is catalyzed by SAT, but a single amino acid change renders the SAT insensitive to feedback inhibition by cysteine that results in cysteine overproduction by the microorganism. Then the excess cysteine is converted into pyruvate, ammonia and sulfide ions by cysteine desulfhydrase. Finally, the secreted sulfide precipitates metal ions like copper and removes it from the solution as copper sulfide nanoparticles. Schaffie and Hosseini (2014) demonstrated in their study that is feasible to produce copper sulfide nanoparticles from acid mine drainage (AMD) through a biological approach. The properties of the produced nanoparticles were the same as the nanoparticles synthesized from the pure copper sulfate solution. These nanoparticles have the same composition like covelite and an average size of 10–40 nm.

### 1.5.5 Silver Sulfide Nanoparticles

Silver sulfide nanoparticles possess unique semi-conducting, optical, and electrical properties and are highly stable. Owing to these features, they are broadly used in solar cell batteries (Tubtimtae et al. 2010), thermoelectric sensors, etc. (Yan et al. 2011). The recently obtained $Ag_2S$/graphene nanocomposite is promising for the development of super capacitors (Mo et al. 2012). The great potential of practical applications of $Ag_2S$ nanoparticles brought into existence numerous protocols for their preparation. The thermolysis of silver xanthates with long aliphatic chains at 200 °C brings about egg shaped particles with a narrow range of sizes (Zhang et al. 2012). Rod shaped $Ag_2S$ nanocrystals have been obtained from silver nitrate and

thioacetamide (Zhao et al. 2007). Lea fshaped $Ag_2S$ nanolayers can be produced by autoclaving an ethanol solution of silver nitrate and carbon disulfide at 160 °C (Chen et al. 2008). Bacteria of the genus *Shewanella* are commonly used in the preparation of nanoparticles of metals, oxides, and sulfides (Perez-Gonzalez et al. 2010). These bacteria can reduce many substances, including metal oxides, nitrates, sulfates, etc. They have been employed in the synthesis of gold nanoparticles (Suresh et al. 2011), arsenic sulfide nanotubes (Jiang et al. 2009), and uranium dioxide nanoparticles (Burgos et al. 2008). Debabova et al. (2013) synthesize $Ag_2S$ nanoparticles using the metal-reducing bacterium *Shewanella oneidensis* MR1 an aqueous solution of $AgNO_3$ and $Na_2S_2O_3$ at an ordinary temperature and pressure. The nanoparticles vary in size within 2–16 nm, and the fraction 6–12 nm in size constitutes about 70 %. The maximum yield of nanoparticles in silver equivalent is 53 %. Being visualized by transmission electron microscopy, the particles look like spheres with average diameters varying from $7 \pm 2$ to $9 \pm 2$ nm. The elemental composition of synthesized nanoparticles has been analyzed by energy dispersive X-ray spectroscopy, and the estimated silver to sulfur atomic ratio is 2:1. The presence of living bacterial cells is mandatory for the formation of $Ag_2S$ nanoparticles in the aqueous salt solution. Changes in the reaction conditions (reagent concentrations, temperature, and cell incubation time in the reaction mixture) influence the yield of nanoparticles dramatically, but have little influence on their size.

### *1.5.6 Zinc Sulfide (ZnS) Nanoparticles*

Zinc sulfide (ZnS), are the most attractive materials for applications in areas such as IR optical devices and fast optical switching devices. Zinc sulfide nanoparticles can be prepared by different methods, such as colloidal aqueous and micellar solution synthesis method (Khiewa et al. 2005), using ultrasonic waves (Behboudnia et al. 2005), microwaves (Ni et al. 2004), and gamma-irradiation (Qiao et al. 2000). In most cases, particles prepared by these methods have some problems including poor reproducibility, control of particle size, distribution and shape. Some reactions require high temperature, and/or high pressure for initiating the reaction, and/or inert atmosphere protection, and/or using toxic matters such as $H_2S$, toxic template and stabilizer, and metallic precursors. When zinc sulfide nanoparticles are used as biological probes in clinic examinations, the synthesis of zinc sulfide is expected to be clean (Dubertret et al. 2002). Consequently, researchers in nanoparticles synthesis have turned to biological systems for inspiration. Spherical aggregates of 2–5 nm sphalerite ZnS particles were formed by sulfate-reducing bacteria under anaerobic conditions (Mandal et al. 2006).

A novel, clean biological transformation reaction by immobilized *Rhodobacter sphaeroides* has been developed for the synthesis of zinc sulfide (ZnS) nanoparticles was developed by Bai et al. (2006). *Rhodobacter sphaeroides* is a purple, non-sulphur, photosynthetic bacterium. It can grow not only aerobically

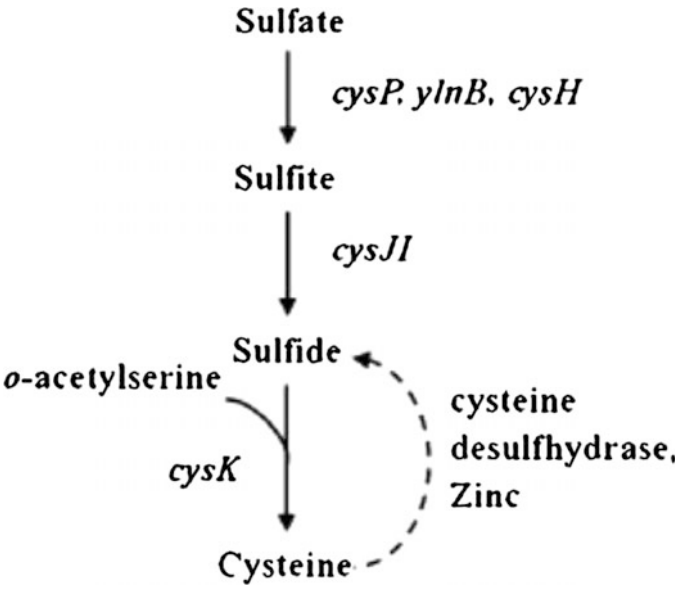


**Fig. 1.18** Sulfate assimilation action of *Rhodobacter sphaeroides*. The enzymes present in *Rhodobacter sphaeroides* are indicated by the corresponding genes: *cys*P, sulfate permease; *yln*B, ATP-sulfurylase; *cys*H, phosphoadenosine phosphosulfate reductase; *cys*JI, sulfite reductase; *cys*K, o-acetylserine synthase. *Source* Bai et al. (2006). Copyright © 2013, Springer. Reproduced with permission

in the dark but also anaerobically in the light and has tolerance to heavy metals (Giotta et al. 2006). In the biological synthetic process for ZnS nanoparticles by *Rhodobacter sphaeroides*, soluble sulfate acts as the source of sulfur. The formation mechanism of ZnS nanoparticles by biological transformation reaction of Rhodobacter sphaeroides can be explained in (Fig. 1.18). First, the soluble sulfate enters into immobilized beads via diffusion, and later is carried to the interior membrane of *Rhodobacter sphaeroides* cell facilitated by sulfate permease Then, the sulfate is reduced to sulfite by ATP sulfurylase and phosphoadenosine phosphosulfate reductase, and next sulfite is reduced to sulfide by sulfite reductase. The sulfide reacts with O-acetylserine to synthesize cysteine via O-acetylserine thiolyase (Holmes et al. 1997; Auger et al. 2005), and then cysteine produces $S^{2-}$ by a cysteine desulfhydrase in presence of zinc. After this process, $S^{2-}$ reacts with the soluble zinc salt and the ZnS nanoparticles are synthesized. Finally, ZnS nanoparticles are discharged from immobilized cells to the solution. In the synthetic process, the particle size is controlled by the culture time of the *Rhodobacter sphaeroides*, and simultaneously the immobilized beads act on separating the ZnS nanoparticles from the *Rhodobacter sphaeroides*. Although the detailed mechanism study of this process is in progress, it suggests that many other high grade binary metal sulfides can also be produced using this method (Bai et al. 2006).

### 1.5.7 Antimony Sulphide ($Sb_2S_3$) Nanoparticles

$Sb_2S_3$ exhibits important applications in photovoltaic, photosensors, optical nanodevices, and photoelectronics. It has been are used in electronics as poor conductors of heat and electricity. Very pure antimony is used to make certain types of semiconductor devices, such as diodes and infrared detectors (Grigorescu and Stradling 2001; Wei et al. 2006). Antimony, as a metallic form, is not soluble in body fluids and, as reported in old literature, cannot produce any effect on human system (Filella et al. 2002a, b). In contrast, organic or inorganic salts of antimony can be decomposed by the fluids and have been used for therapeutic purposes (Filella et al. 2002a, b; Johnson et al. 2005). Antimony salts are currently chosen for the treatment of leishmaniasis, a disease that affects 12 million people annually around the world (Berman 1997; Haldar et al. 2011). Moreover, trivalent antimony compounds have been used in treating bilharzia, trypanosomiasis and kala-azar for more than a century (Berman 1997; Isago et al. 2008).

Bahrami et al. (2012) explored the biological synthesis of antimony sulfide using *Serratia marcescens*. The bacterium was isolated from the Caspian Sea in northern Iran and was used for intracellular biosynthesis of antimony sulfide nanoparticles. This isolate was identified as nonpigmented *Serratia marcescens* using conventional identification assays and the 16S rDNA fragment amplification method, and was used to prepare inorganic antimony nanoparticles. Antimony-supplemented nutrient agar (NA) plates ($SbCl_3$, 1 % w/v) were inoculated with the bacterial isolate. These inoculated NA media were incubated aerobically at 30 °C. After 72 h, bacterial cells were harvested from the surface of culture media. The biogenic nanoparticles were released by liquid nitrogen and extracted using two sequential solvent extraction systems. The energy-dispersive x-ray demonstrated that the extracted nanoparticles consisted of antimony and sulfur atoms. The transmission electron micrograph showed the small and regular non-aggregated nanoparticles ranging in size less than 35 nm. Although the chemical synthesis of antimony sulfide nanoparticles has been reported in the literature, the biological synthesis of antimony sulfide nanoparticles has not previously been published. This is the first report to demonstrate a biological method for synthesizing inorganic nanoparticles composed of antimony (Bahrami et al. 2012).

## 1.6 Palladium and Platinum Nanoparticles

Palladium is an excellent hydrogenation and dehydrogenation catalyst available in organo-metallic forms. Palladium nanoparticles have found to be effective catalysts in a number of chemical reactions due to their increased surface area over the bulk metal. The sulfate-reducing bacterium, *Desulfovibrio desulfuricans* and metal iron-reducing bacterium, *Shewanella oneidensis*, were capable of reducing soluble

palladium (II) into insoluble palladium (0) with formate, lactate, pyruvate, or $H_2$ as the electron donor (Lloyd et al. 1998; Yong et al. 2002a; de Windt et al. 2005).

Coker et al. (2010) demonstrated a novel biotechnological route for the synthesis of heterogeneous catalyst, consisting of reactive palladium nanoparticles arrayed on a nanoscale biomagnetite support. The magnetic support was synthesized at ambient temperature by the Fe (III)-reducing bacterium *Geobacter sulfurreducens*. The palladium nanoparticles were deposited on the nanomagnetite using simple one-step method to an organic coating priming the surface for Pd adsorption, which was produced by the bacterial culture during the formation of the nanoparticles. A recent biological method used to produce palladium nanoparticles is the precipitation of Pd on a bacterium. These palladium nanoparticles can be applied as catalyst in dehalogenation reactions. Large amounts of hydrogen are required as electron donors in these reactions, resulting in considerable cost. A study carried out by Hennebel et al. (2011) demonstrates how bacteria is cultivated under anaerobic conditions and can be used to reductively precipitate the palladium catalysts and generate the hydrogen (electron donor). This avoids the cost coupled to hydrogen supply. Batch reactors with nanoparticles formed by *Citrobacter braakii* showed the highest diatrizoate dehalogenation (Hennebel et al. 2011).

Konishi et al. (2007b) demonstrated that resting cells of *Shewanella algae* were able to deposit platinum NPs by reducing $PtCl_6^{2-}$ ions within 60 min at pH 7 and 25 °C. Biogenic platinum NPs of about 5 nm were located in the periplasmic space. In this case, the cell suspension changed the color from pale yellow to black in 10 min. The black appearance provided a convenient visible signature for the microbial formation of metallic platinum NPs. The observed decrease in aqueous platinum concentration was presumably caused by the rapid reduction of $PtCl_6^{2-}$ ions into insoluble platinum. In the absence of lactate, however, *S. algae* cells were not able to reduce the $PtCl_6^{2-}$ ions. They reported that the $PtCl_6^{2-}$ ions were not chemically reduced by lactate. Yong et al. (2002b) also reported that the sulfate-reducing bacterium *Desulfovibrio desulfuricans* was able to adsorb only 12 % of platinum (IV) ions on the bacterial cells from 2 mM platinum chloride solution. In another study, Gram-negative cyanobacterium, *Pediastrum boryanum* UTEX 485, extracellularly produced Pt (II)-organics and metallic platinum NPs at 25–100 °C for up to 28 days and 180 °C for 1 day with different morphologies of spherical, bead-like chains and dendritic in the size range of 30 nm–0.3 μm (Lengke et al. 2006c).

## 1.7 Selenium Tellurium Nanoparticles

Selenium is of considerable environmental importance as it is essential at low concentrations but toxic at high concentrations for animals and humans, with a relatively small difference between these values (Fordyce 2005). Selenium occurs in different oxidation states as reduced form (selenide, $Se^{2-}$), least mobile elemental selenium ($Se^0$) and water soluble selenite ($SeO_3^2$)/selenate ($SeO_4^2$) oxyanions.

Selenium possesses several applications in medicine, chemistry and electronics. Selenium (Se), as a functional material, is an important semiconductor and photoelectric element due to its special physical properties (Zhang et al. 2011). Therefore, Se is used in many applications ranging from photocells, photographic exposure meters and solar cells to semiconductor rectifiers. Recently, there has been increasing interest in the synthesis of nanoparticles using microorganisms, leading to the development of various biomimetic approaches (Mohampuria et al. 2008). However, most methods used to synthesize SeNPs are characterized by elevated temperatures and high pressures and are hazardous to the environment (Zhang et al. 2011).

*Stenotrophomonas maltophilia* SELTE02 showed promising transformation of selenite ($SeO_3^{-2}$) to elemental selenium ($Se^0$) accumulating selenium granules either in the cell cytoplasm or in the extracellular space. In addition, *Enterobacter cloacae* SLD1a-1, *Rhodospirillum rubrum*, and *Desulfovibrio desulfuricans* have also been found to bioreduce selenite to selenium both inside and outside the cell with various morphologies like spherical, fibrillar, and granular structure or with small atomic aggregates. *E. coli* also deposited elemental selenium both in periplasmic space and cytoplasm, and *P. stutzeri* also aerobically reduced selenite to elemental selenium (Narayanan and Sakthivel 2010). Under aerobic conditions, Hunter and Manter (2008) reported that *Tetrathiobacter kashmirensis* bioreduced selenite to elemental red selenium. A 90-kDa protein present in the cell-free extract was believed to be responsible for this bioreduction. Moreover, Yadav et al. (2008) showed that *P. aeruginosa* SNT1 biosynthesized nanostructured selenium by biotransforming selenium oxyanions to spherical amorphous allotropic elemental red selenium both intracellularly and extracellularly.

Oremland et al. (2004) reported the biogenesis of SeNPs under anaerobic conditions. $Se^0$ nanoparticles (SeNPs) formed by the Se-respiring bacteria, such as *Sulfurospirillum barnesii*, *Bacillus selenitireducens*, and *Selenihalanaerobacter shriftii*, are structurally unique when compared to $Se^0$ formed by chemical synthesis. However, anaerobic conditions have limitations, such as culture conditions and isolate characteristics that make biosynthesis processes tedious and challenging (Prakash et al. 2009). The generation of SeNPs by soil bacteria *Pseudomonas aeruginosa* and *Bacillus* sp. under aerobic conditions has been reported; however, these studies only include the partial characterization of selenium nanospheres (Yadav et al. 2008; Prakash et al. 2009). The characterization of the nanospheres in relation to size is of great importance, both in industrial and biologic activities. Recent reports describe that $Se^0$ nanoparticles with a size under 100 nm have a greater bioavailability (Thakkar et al. 2009; Dhanjal and Cameotra 2010). In addition, other studies mention that a smaller size increases the ability to trap free radicals with greater antioxidant effect (Huang et al. 2003). Peng et al. (2007) mentioned that the size of $Se^0$ nanoparticles plays an important role in their biologic activity and, as expected, 5–200 nm nano-Se can directly scavenge free radicals in vitro in a size dependent fashion. The bio-reduction of selenite (Se [IV]) by *Pantoea agglomerans* generates nanoparticles with sizes ranging between 30 and 300 nm was reported by Torres et al. (2012). Their study demonstrated that,

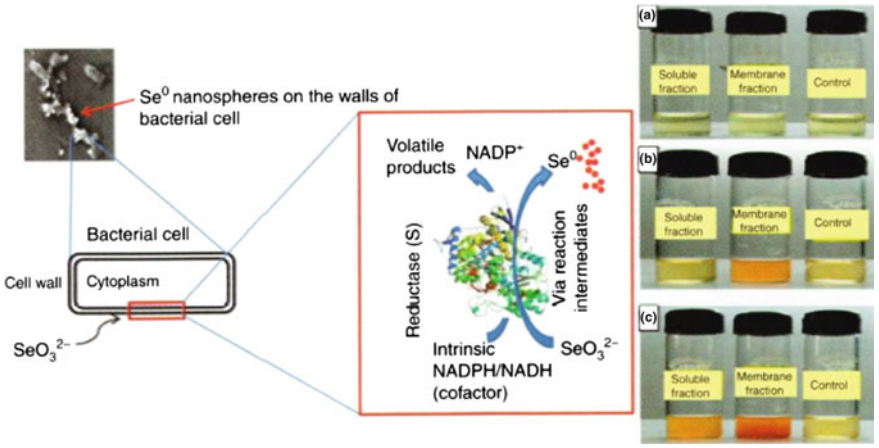


**Fig. 1.19** Proposed mechanism for biogenesis of selenium nanospheres at different time intervals: **a** selenite reduction at 0 h; **b** formation of red elemental selenium in membrane fraction after 3–4 h of incubation; and **c** insoluble fraction after 12 h of incubation. *Source* Dhanjal and Cameotra (2010). Copyright © 2010, BioMed Central. Reproduced with permission

*Pantoea agglomerans* strain UC-32 produce amorphous SeNPs under aerobic conditions with a size optimal for biotechnological use (such as trapping free radicals in the induction of selenoenzymes) after at least 20 h of incubation. These results are of great importance due to the low culture requirements of UC-32 strain with the subsequent low cost of biologically active SeNPs production.

Synthesis of $S^0$ under aerobic conditions by *Bacillus cereus* was investigated by Dhanjal and Cameota (2010). The aerobic reduction of selenate ($SeO_4^{2-}$) and selenite ($SeO_3^{2-}$) to $Se^0$ is depicted in Fig. 1.19. The electron transfer was initiated from NADPH/NADH by NADPH/NADH-dependent electron carrier. The results show: (1) selenite reduction in 0 h; (2) formation of red elemental selenium in membrane fraction after 3–4 h of incubation; and (3) prolonged incubation for 12 h resulted in formation of red elemental selenium in soluble fraction.

Tellurium (Te) has been reduced from tellurite to elemental tellurium by two anaerobic bacteria, *Bacillus selenitireducens* and *Sulfurospirillum barnesii*. *B. selenitireducens* initially formed nanorods of 10 nm in diameter and 200 nm in length were clustered together to form larger rosettes of $\sim$1000 nm but with *S. barnesii* small irregularly shaped extracellular nanospheres of diameter <50 nm were formed (Baesman et al. 2007). In another study, tellurium-transforming *Bacillus* sp. BZ isolated from the Caspian Sea in northern Iran was used for the intracellular biosynthesis of elemental tellurium NPs. The biogenic NPs were released by liquid nitrogen and purified by an n-octyl alcohol water extraction system. TEM analysis showed rod-shaped NPs with dimensions of about 20 × 180 nm. The produced NPs had a hexagonal crystal structure (Zare et al. 2012).

## 1.8 Bismuth Nanoparticles

The bismuth nanoparticles (BiNPs) has attracted a great deal of interest because of its potential applications in X-ray radiation therapy, catalysts, thermoelectricity, and optical uses (Hossain and Su 2012; Wang and Buhro 2010; Carotenuto et al. 2009; Lin et al. 2011). BiNPs electrodes have been applied in the detection of heavy metal ions as a substitute for bismuth film (Sahoo et al. 2013) In addition, bismuth compounds, such as $BiPO_4$ (Pan et al. 2010), $BiVO_4$ (Qu et al. 2013), $Bi_2O_3$, (Zhou et al. 2009) and $Bi_2S_3$ nanoparticles (Wu et al. 2010b) were also reported over the past decades as novel catalysts for photodegradation of environmental pollutants. Several approaches have been employed to fabricate BiNPs including thermal plasma (Wang et al. 2007) an electrochemical method (Reim et al. 2013) a gas condensation method (Lee et al. 2007) and solution phase chemical methods. The latter is the most popular method, which often involves the reduction of relevant metal salts with various reductants in the presence of morphology-controlling surfactants.

The biological synthesis of BiNPs was explored using *Serratia marcescens* by Nazari et al. (2012). The biogenic bismuth NPs were released by liquid nitrogen and purified using an n-octanol water two-phase extraction system. The energy-dispersive X-ray and X-ray diffraction (XRD) patterns demonstrated that the purified NPs consisted of only bismuth and are amorphous. In addition, the transmission electron micrograph showed that the small NPs formed larger aggregated NPs around 150 nm.

## 1.9 Conclusions and Future Perspectives

Biological systems; bacteria, fungi, actinomycetes, and algae have many opportunities for utilization in nanotechnology, especially in the development of a reliable and eco-friendly processes for the synthesis of metallic nanoparticles. The rich microbial diversity points to their innate potential for acting as potential biofactories for nanoparticles synthesis. Despite some related reports, many aspects of nanoparticles biosynthesis remain unclear especially with regards to why and how the size and shapes of the synthesized nanoparticles are influenced by the biological systems. The biochemical and molecular mechanisms of biosynthesis of metallic nanoparticles need to be better understood to improve the rate of synthesis and monodispersity of the product. The properties of NPs can be controlled by optimization of important parameters which control the growth condition of organisms, cellular activities, and enzymatic processes (optimization of growth and reaction conditions). The large-scale synthesis of NPs using microorganisms is interesting because it does not need any hazardous, toxic, and expensive chemical materials for synthesis and stabilization processes. It seems that by optimizing the reaction conditions and selecting the best microbes, these natural nanofactories can be used in the synthesis of stable NPs with well-defined sizes, morphologies, and compositions.

## References

Absar A, Satyajyoti S, Khan MI, Rajiv K, Sastry M (2005) Extra/intracellular biosynthesis of gold nanoparticles by an alkalotolerant fungus, *Trichothecium* sp. J Biomed Nanotechnol 1:47–53

Ahmad A, Mukherjee P, Mandal D, Senapati S, Khan MI, Kumar R, Sastry M (2002) Enzyme mediated extracellular synthesis of CdS nanoparticles by the fungus, *Fusarium oxysporum*. J Am Chem Soc 124:12108–12109

Ahmad A, Mukherjee P, Senapati S, Mandal D, Khan MI, Kumar R, Sastry M (2003a) Extracellular biosynthesis of silver nanoparticles using the fungus *Fusarium oxysporum*. Colloids Surf B 28:313–318

Ahmad A, Senapati S, Khan MI, Ramani R, Srinivas V, Sastry M (2003b) Intracellular synthesis of gold nanoparticles by a novel alkalotolerant actinomycete, *Rhodococcus* species. Nanotechnology 14:824–828

Agnihotri M, Joshi S, Kumar AR, Zinjarde S, Kulkarni S (2009) Biosynthesis of gold nanoparticles by the tropical marine yeast *Yarrowia lipolytica* NCIM 3589. Mater Lett 63:1231–1234

Acharya BK (1972) Elementary pharmacology and therapeutics. New Height Publishing, New Delhi, pp 154–155

Argyo C, Weiss V, Bräuchle C, Bein T (2014) Multifunctional mesoporous silica nanoparticles as a universal platform for drug delivery. Chem Mater 26:435–451

Arumugam A, Karthikeyan C, Hameed ASH, Gopinath K, Gowri S, Karthika V (2015) Synthesis of cerium oxide nanoparticles using *Gloriosa superba* L. leaf extract and their structural, optical and antibacterial properties. Mat Sci Eng C 49:408–415

Auger S, Gomez MP, Danchin A, Martin-Verstraete I (2005) The PatB protein of *Bacillus subtilis* is aC-S-lyase. Biochimie 87:231–238

Ayano H, Miyake M, Terasawa K, Kuroda M, Soda S, Sakaguchi T, Ike M (2014) Isolation of a selenite-reducing and cadmium-resistant bacterium *Pseudomonas* sp. strain RB for microbial synthesis of CdSe nanoparticles. J Biosci Bioeng 117:576–581

Babu MMG, Gunasekaran P (2009) Production and structural characterization of crystalline silver nanoparticles from *Bacillus cereus* isolate. Colloids Surf B 74:191–195

Bai HJ, Zhang ZM (2009) Microbial synthesis of semiconductor lead sulfide nanoparticles using immobilized *Rhodobacter sphaeroides*. Mater Lett 63:764–766

Bai HJ, Zhang ZM, Gong J (2006) Biological synthesis of semiconductor zinc sulfide nanoparticles by immobilized *Rhodobacter sphaeroides*. Biotechnol Lett 28:1135–1139

Bai HJ, Zhang ZM, Guo Y, Yang GE (2009) Biosynthesis of cadmium sulfide nanoparticles by photosynthetic bacteria *Rhodopseudomonas palustris*. Colloids Surf B Biointerfaces 70: 142–146

Bansal V, Rautaray D, Ahmad A, Sastry M (2004) Biosynthesis of zirconia nanoparticles using the fungus *Fusarium oxysporum*. J Mater Chem 14(22):3303–3305

Bansal V, Rautaray D, Bharde A, Ahire K, Sanyal A, Ahmad A, Sastryet M (2005) Fungus-mediated biosynthesis of silica and titania particles. J Mater Chem 15:2583–2589

Bansal V, Poddar P, Ahmad A, Sastry M (2006) Room temperature biosynthesis of ferroelectric barium titanate nanoparticles. J Am Chem Soc 128:11958–11963

Bao H, Lu Z, Cui X, Qiao Y, Guo J, Anderson JM, Li CM (2010) Extracellular microbial synthesis of biocompatible CdTe quantum dots. Acta Biomater 6:3534–3541

Baesman SM, Bullen TD, Dewald J, Zhang D, Curran S, Islam FS, Beveridge TJ, Oremland RS (2007) Formation of tellurium nanocrystals during anaerobic growth of bacteria that use Te oxyanions as respiratory electron acceptors. Appl Environ Microbiol 73:2135–2143

Bahrami K, Nazari P, Sepehrizadeh Z, Zarea B, Shahverdi AR (2012) Microbial synthesis of antimony sulfide nanoparticles and their characterization. Ann Microbiol 62:1419–1425

Bazylinski DA, Frankel RB, Heywood BR, Mann S, King JW, Donaghay PL, Hanson AK (1995) Controlled biomineralization of magnetite ($Fe_3O_4$) and greigite ($Fe_3S_4$) in a magnetotactic bacterium. Appl Environ Microbiol 61:3232–3239

Bhainsa KC, D'Souza SF (2006) Extracellular biosynthesis of silver nanoparticles using the fungus *Aspergillus fumigatus*. Colloid Surf B 47:160–164

Bharde A, Wani A, Shouche Y, Pattayil A, Bhagavatula L, Sastry M (2005) Bacterial aerobic synthesis of nanocrystalline magnetite. J Am Chem Soc 127:9326–9327

Bharde AA, Parikh RY, Baidakova M, Jouen S, Hannoyer B, Enoki T, Prasad BLV, Shouche YS, Ogale S, Sastry M (2008) Bacteria-mediated precursor-dependent biosynthesis of superparamagnetic iron oxide and iron sulfide nanoparticles. Langmuir 24:5787–5794

Behboudnia M, Majlesara MH, Khanbabaee B (2005) Preparation of ZnS nanorods by ultrasonic waves. Mater Sci Eng B 122:160–163

Berman JD (1997) Human leishmaniasis: clinical, diagnostic, and chemotherapeutic developments in the last 10 years. Clin Infect Dis 24:684–703

Bond GC (2002) Gold: a relatively new catalyst. Catal Today 72:5–9

Bondarenko O, Juganson K, Ivask A, Kasemets K, Mortimer M, Kahru A (2013) Toxicity of Ag, CuO and ZnO nanoparticles to selected environmentally relevant test organisms and mammalian cells in vitro: a critical review. Arch Toxicol 87:1181–1200

Bose S, Hochella MF, Gorby YA, Kennedy DW, McCready DE, Madden AS, Lower BH (2009) Bioreduction of hematite nanoparticles by the dissimilatory iron reducing bacterium *Shewanella oneidensis* MR-1. Geochim et Cosmochim Acta 73:962–976

Burgos WD, McDonongh JT, Senko JM, Zhang G, Dohnalkova AC, Kekky SD, Gorby Y, Kenner KM (2008) Characterization of uraninite nanoparticles produced by *Shewanella oneidensis* MRI. Geochim Cosmochim Acta 72:4901–4915

Carotenuto G, Hison CL, Capezzuto F, Palomba M, Perlo P, Conte P (2009) Synthesis and thermoelectric characterisation of bismuth nanoparticles. J Nanopart Res 11:1729–1738

Castro-Longoria E, Vilchis-Nestor AR, Avalos-Borja M (2011) Biosynthesis of silver, gold and bimetallic nanoparticles using the filamentous fungus *Neurospora crassa*. Coll Surf B 83: 42–48

Chauhan A, Zubair S, Tufail S, Shherwani S, Sajid M, Raman SC, Azam A (2011) Fungus-mediated biological synthesis of gold nanoparticles: potential in detection of liver cancer. Int J Nanomed 6:2305–2319

Chen R, Nufter NNT, Moussa L, Morris HK, Whitemore PM (2008) Silver sulfide nanoparticles assembly obtained by reaction an assembled silver nanoparticles template with hydrogen sulfide gas. Nanotechnology 19:45604–45915

Chwalibog A, Sawosz E, Hotowy A, Szeliga J, Mitura S, Mitura K, Grodzik M, Orlowski P, Sokolowska A (2010) Visualization of interaction between inorganic nanoparticles and bacteria or fungi. Int J Nanomed 5:1085–1094

Coker VS, Bennett JA, Telling DD, Henkel T, Charnock JM, van der Laan G, Pattrick RA, Pearce CI, Cutting RS, Shannon IJ, Wood J, Arenholz E, Lyon IC, Lloyd JR (2010) Microbial engineering of nanoheterostructures: biological synthesis of a magnetically recoverable palladium nanocatalyst. ACS Nano 4:2577–2584

Cornell A, Schwertmann U (2003) The iron oxides: structures, properties, reactions, occurrences and used. Wiley, New York, Weinheim, p 664

Cuevas N, Durán M, Diez C, Tortella GR, Rubilar O (2015) Extracellular biosynthesis of copper and copper oxide nanoparticles by *Stereum hirsutum*, a native white-rot fungus from chilean forests. J Nanomater. Article ID 789089, 1–7.

Cui R, Liu HH, Xie HY, Zhang ZL, Yang YR, Pang DW, Xie ZX, Chen BB, Hu B, Shen P (2009) Living yeast cells as a controllable biosynthesizer for fluorescent quantum dots. Adv Funct Mater 19:2359–2364

Cunningham DP, Lundie LL Jr (1993) Precipitation of cadmium by *Clostridium thermoaceticum*. Appl Environ Microbiol 59:7–14

Dahle JT, Arai Y (2015) Environmental geochemistry of cerium: applications and toxicology of cerium oxide nanoparticles. Int J Environ Res Public Health 12:1253–1278

Dameron CT, Reese RN, Mehra RK, Kortan AR, Carooll PJ, Steigerwald ML, Brus LE, Winge DR (1989) Biosynthesis of cadmium sulphide quantum semiconductor crystallites. Nature 338:596–597

Daniel MC, Astruc D (2004) Gold nanoparticles: assembly, supramolecular chemistry, quantum-size-related properties, and applications toward biology, catalysis, and nanotechnology. Chem Rev 104:293–346

de Windt W, Aelterman P, Verstraete W (2005) Bioreductive deposition of palladium (0) nanoparticles on *Shewanella oneidensis* with catalytic activity towards reductive dechlorination of polychlorinated biphenyls. Environ Microbiol 7:314–325

Debabova VG, Voeikova TA, Shebanova AS, Shaitanb KV, Emel'yanova LK, Novikova LM, Kirpichnikov MP (2013) Bacterial synthesis of silver sulfide nanoparticles. Nanotechnol Russ 8:269–276

Dhanjal S, Cameotra S (2010) Aerobic biogenesis of selenium nanospheres by *Bacillus cereus* isolated from coalmine soil. Microb Cell Fact 9:1–11

Dubertret B, Skourides P, Norris DJ, Noireaux V, Brivanlou AH, Libchaber A (2002) In vivo imaging of quantum dots encapsulated in phospholipid micelles. Science 298:1759–1762

El-Rafie HM, El-Rafie HM, Zahran MK (2013) Green synthesis of silver nanoparticles using polysaccharides extracted from marine macroalgae. Carbohydr Polym 96:403–410

El-Shanshoury AERR, Elsilk SE, Ebeid ME (2012) Rapid biosynthesis of cadmium sulfide (CdS) nanoparticles using culture supernatants of *Escherichia coli* ATCC 8739, *Bacillus subtilis* ATCC 6633 and *Lactobacillus acidophilus* DSMZ 20079T. Afr J Biotechnol 11: 7957–7965

Eshed M, Pol S, Gedanken A, Balasubramanian M (2011) Zirconium nanoparticles prepared by the reduction of zirconium oxide using the RAPET method Beilstein. J Nanotechnol 2: 198–203

Faramazi MA, Sadighi A (2013) Insights into biogenic and chemical production of inorganic nanomaterials and nanostructures. Adv Colloid Interface Sci 189–190:1–20

Fayaz AM, Balaji K, Girilal M, Yadav R, Kalaichelvan PT, Venketesan R (2010) Biogenic synthesis of silver nanoparticles and their synergistic effect with antibiotics: a study against gram-positive and gram-negative bacteria. Nanomed: Nanotechnol Biol Med 6:103–109

Filella M, Belzile N, Chen YW (2002a) Antimony in the environment: a review focused on natural waters: I. Occurrence. Earth Sci Rev 57:125–176

Filella M, Belzile N, Chen YW (2002b) Antimony in the environment: a review focused on natural waters: II. relevant solution chemistry. Earth Sci Rev 59:265–285

Fordyce FM (2005) Selenium deficiency and toxicity in the environment. In: Selinus O, Alloway B, Centeno JA, Finkelman RB, Fuge R, Lindh U, Smedley P (eds) Essentials of medical geology. Elsevier Academic Press, Amsterdam, pp 373–416

Friedrichs S, Meyer RR, Sloan J, Kirkland AI, Hutchison JI, Green MLH (2001) Complete characterization of a $Sb_2O_3$/(21,-8)SWNP inclusion composites. Chem Commun 10:929–930

Gadd GM (2010) Metals, minerals and microbes: geomicrobiology and bioremediation. Microbiology 156:609–643

Gaumet M, Vargas A, Gurny R, Delie F (2008) Nanoparticles for drug delivery: the need for precision in reporting particle size parameters. Eur J Pharm Biopharm 69:1–9

Gericke M, Pinches A (2006) Biological synthesis of metal nanoparticles. Hydrometallurgy 83:132–140

Giotta L, Agostiano A, Italiano F, Milano F, Trotta M (2006) Heavy metal ion influence on the photosynthetic growth of *Rhodobacter sphaeroides*. Chemosphere 62:1490–1499

Goel S, Chen F, Cai W (2014) Synthesis and biomedical applications of copper sulfide nanoparticles: from sensors to theranostics. Small 4:631–645

Gong XQ, Selloni A (2005) Reactivity of anatase $TiO_2$ nanoparticles: the role of the minority (001) surface. J Phys Chem B 109:19560–19562

Grigorescu CEA, Stradling RA (2001) Antimony-based infrared materials and devices. Thin Films 28:147–191

Guo L, Wu Z, LiuT Wang W, Zhu H (2000) Synthesis of novel $Sb_2O_3$ nanorods. Chem Phys Lett 318:49–52

Gurunathan S, Kalishwaralal K, Vaidyanathan R, Venkataraman D, Pandian SR, Muniyandi J, Hariharan N, Eom SH (2009) Biosynthesis, purification and characterization of silver nanoparticles using *Escherichia coli*. Colloids Surf B 74:328–335

Haldar AK, Sen P, Roy S (2011) Use of antimony in the treatment of leishmaniasis. current status and future directions. Mol Biol Int. Article ID 571242, 23 p

Harada M, Asakura K, Toshima N (1993) Catalytic activity and structural analysis of polymer-protected gold/palladium bimetallic clusters prepared by the successive reduction of hydrogen tetrachloroaurate(III) and palladium dichloride. J Phys Chem 97:5103–5114

He S, Guo Z, Zhang Y, Zhang S, Wang J, Gu N (2007) Biosynthesis of gold nanoparticles using the bacteria *Rhodopseudomonas capsulata*. Mater Lett. 61:3984–3987

Hennebel T, Nevel S, Verschuere S, De Corte S, De Gusseme B, Cuvelier C, Fitts JF, van der Lelie D, Boon N, Verstraeteet W (2011) Palladium nanoparticles produced by fermentatively cultured bacteria *Rhodopseudomonas capsulate*. Mater Lett 61:3984–3987

Holmes JD, Richardson DJ, Saed S, Evans-Gowing R, Russell DA, Sodeau JR (1997) Cadmium-specific formation of metal sulfide "Q-particle" by *Klebsiella pneumoniae*. Microbiology 143:2521–2530

Holt KB, Bard AJ (2005) Interaction of silver(I) ions with the respiratory chain of *Escherichia coli*: an electrochemical and scanning electrochemical microscopy study of the antimicrobial mechanism of micromolar Ag. Biochemistry 44:13214–13223

Honary S, Barabadi H, Gharaei-Fathabad E, Naghibi F (2012) Green synthesis of copper oxide nanoparticles using *Penicillium aurantiogriseum*, *Penicillium citrinum* and *Penicillium waksmani*. Dig J Nanomater Bios 7:999–1005

Hossain M, Su M (2012) Nanoparticle location and material dependent dose enhancement in X-ray radiation therapy. J Phys Chem 116:23047–23052

Hosseini M, Schaffie M, Pazouki M, Darezereshki E, Ranjbar M (2012) Biologically synthesized copper sulfide nanoparticles: production and characterization. Mater Sci Semicond Process 15:222–225

Huang B, Zhang J, Hou J, Chen C (2003) Free radical scavenging efficiency of Nano-Se in vitro. Free Radical Biol Med 35:805–813

Hunter WJ, Manter DK (2008) Bio-reduction of selenite to elemental red selenium by *Tetrathiobacter kashmirensis*. Curr Microbiol 57:83–88

Husseiny MI, El-Aziz AM, Badr Y, Mahmoud MA (2007) Biosynthesis of gold nanoparticles using *Pseudomonas aeruginosa*. Spectrochim Acta Part A 67:1003–1006

Isago H, Miura K, Oyama Y (2008) Synthesis and properties of a highly soluble dihydoxo (tetra-tert-butylphthalocyaninato) antimony(V) complex as a precursor toward water-soluble phthalocyanines. J Inorg Biochem 102:380–387

Jain A, Bhargava S, Majumdar J, Tarafdar C, Panwar J (2011) Extracellular biosynthesis and characterization of silver nanoparticles using *Aspergillus flavus* NJP08: a mechanism perspective. Nanoscale. 3:635–641

Jayaseelan C, Rahuman AA, Kirthi AV, Marimuthu S, Santhoshkumar T, Bagavan A, Gaurav K, Karthik L, Rao KV (2012) Novel microbial route to synthesize ZnO nanoparticles using *Aeromonas hydrophila* and their activity against pathogenic bacteria and fungi. Spectrochim Acta A: Mol Biomol Spectrosc 90:78–84

Jha AK, Prasad K (2010) Ferroelectric $BaTiO_3$ nanoparticles: biosynthesis and characterization. Colloids Surf B 75:330–334

Jha AK, Prasad K, Kulkarni AR (2009a) Synthesis of $TiO_2$ nanoparticles using microorganisms. Colloids Surf B 71:226–229

Jha AK, Prasad K, Prasad K (2009b) A green low-cost biosynthesis of $Sb_2O_3$ nanoparticles. Biochem Eng J 43:303–306

Jiang S, Lee JH, Kim MG, Mynng NV, Fredrickson JK, Sadowsky MJ, Hur HG (2009) Biogenic formation of AsS nanotubes by diverse *Shewanella* strains. Appl Environ Microbiol 75: 6896–6898

Jiang XM, Wang LM, Wang J, Chen CY (2012) Gold nanomaterials: preparation, chemical modification, biomedical applications and potential risk assessment. Appl Biochem Biotechnol 166:1533–1551

Jianping X, Jim YL, Daniel ICW, Yen PT (2007) Identification of active biomolecules in the high-yield synthesis of single-crystalline gold nanoplates in algal solutions. Small 3:668–672

Johnson CA, Moench H, Wersin P, Kugler P, Wenger C (2005) Solubility of antimony and other elements in samples taken from shooting ranges. J Environ Qual 34:248–254

Juibari MM, Abbasalizadeh S, Jouzani GS, Noruzi M (2011) Intensified biosynthesis of silver nanoparticles using a native extremophilic *Ureibacillus thermosphaericus* strain. Mater Lett 65:1014–1017

Kalabegishvili TL, Kirkesali EL, Rcheulishvili AN, Ginturi EN, Murusidze IG, Pataraya DT, Gurielidze MA, Tsertsvadze GI, Gabunia VN, Lomidze LG, Gvarjaladze DN, Frontasyeva N (2012) Synthesis of gold and silver nanoparticles by some microorganisms. Nano Stud 6:5–14

Kalimuthu K, Suresh Babu R, Venkataraman D, Bilal M, Gurunathan S (2008) Biosynthesis of silver nanocrystals by *Bacillus licheniformis*. Colloids Surf B 65:150–153

Kalishwaralal K, Deepak V, Ram Kumar Pandian S, Kottaisamy M, BarathmaniKanth S, Kartikeyan B, Gurunathan S (2010) Biosynthesis of silver and gold nanoparticles using *Brevibacterium casei*. Colloids Surf B 77:257–262

Kang SH, Bozhilov KN, Myung NV, Mulchandani A, Chen W (2008) Microbial synthesis of CdS nanocrystals in genetically engineered *E. coli*. Angew Chem Int Ed 47:5186–5189

Kapoor S, Lawless D, Kennepohl P, Meisel D, Serpone N (1994) Reduction and aggregation of silver ions in aqueous gelatine solutions. Langmuir 10:3018–3022

Kashefi K, Lovley DR (2000) Reduction of Fe(III), Mn(IV), and toxic metals at 100°C by *Pyrobaculum islandicum*. Appl Environ Microbiol 66:1050–1056

Kato H (2011) In vitro assays: tracking nanoparticles inside cells. Nat Nanotechnol 6:139–140

Khiewa PS, Radimana S, Huanga NM, Ahmada MS, Nadarajah K (2005) Preparation and characterization of ZnS nanoparticles synthesized from chitosan laurate micellar solution. Mater Lett 59:989–993

Kirthi AV, Rahuman AA, Rajakumar G, Marimuthu S, Santhoshkumar T, Jayaseelan C, Elango G, Zahir AA, Kamaraj C, Bagavan A (2011) Biosynthesis of titanium dioxide nanoparticles using bacterium *Bacillus subtilis*. Mater Lett 65:2745–2747

Klaus T, Joerger R, Olsson E, Granqvist CG (1999) Silver-based crystalline nanoparticles, microbially fabricated. Proc Natl Acad Sci USA 96:13611–13614

Konishi Y, Ohno K, Saitoh N, Nomura T, Nagamine S (2004) Microbial synthesis of gold nanoparticles by metal reducing bacterium. Trans Mater Res Soc Jpn 29:2341–2443

Konishi Y, Tsukiyama T, Tachimi T, Saitoh N, Nomura T, Nagamine S (2007a) Microbial deposition of gold nanoparticles by the metal-reducing bacterium *Shewanella algae*. Electrochim Acta 53:186–192

Konishi Y, Ohno K, Saitoh N, Nomura T, Nagamine S, Hishida H, Takahashi Y, Uruga T (2007b) Bioreductive deposition of platinum nanoparticles on the bacterium *Shewanella algae*. J Biotechnol 128:648–653

Kowshik M, Deshmuke N, Vogal W, Urban J, Kulkarni SK, Paknikar KM (2002) Microbial synthesis of semiconductor CdS nanoparticles, their characterization, and their use in the fabrication of an ideal diode. Biotechnol Bioeng 78:583–588

Kumar SA, Ansary AA, Ahmad A, Khan MI (2007) Extracellular biosynthesis of CdSe quantum dots by fungus, *Fusarium oxysporum*. J Biomed Nanotechnol 3:190–194

Labrenz M, Druschel GK, Thomsen-Ebert T, Gilbert B, Welch SA, Kemner KM, Logan GA, Summons RE, De Stasio G, Bond PL, Lai B, Kelly SD, Banfield JF (2000) Formation of sphalerite (ZnS) deposits in natural biofilms of sulfate-reducing bacteria. Science 290: 1744–1747

Lai JCK, Lai MB, Edgley KL, BhushanA, Dukhande V, Daniels CK, Leung SW (2007a) Silicon dioxide nanoparticles can exert cytotoxic effects on neural cells. Chapter 8: bio materials and tissues. In: Proceedings of 2007 nanotechnology conference and trade show, Vol 2, pp 741–743

Lai JCK, Schoen MP, Perez Gracia A, Naidu DS, Leung SW (2007b) Prosthetic devices: challenges and implications of robotic implants and biological interfaces. Proc Inst Mech Eng H 221:173–183

Lee GJ, Lee HM, Rhee CK (2007) Bismuth nano-powder electrode for trace analysis of heavy metals using anodic stripping voltammetry. Electrochem Commun 9:2514–2518

Lengke MF, Fleet ME, Southam G (2006a) Morphology of gold nanoparticles synthesized by filamentous cyanobacteria from gold(I)-thiosulfate and gold(III)-chloride complexes. Langmuir 22:2780–2787

Lengke MF, Ravel M, Fleet ME, Wanger G, Gordon RA, Southam G (2006b) Mechanisms of gold bioaccumulation by filamentous cyanobacteria from gold(III)-chloride complex. Environ Sci Technol 40:6304–6309

Lengke MF, Fleet ME, Southam G (2006c) Synthesis of platinum nanoparticles by reaction of filamentous cyanobacteria with platinum(IV)-chloride complex. Langmuir 22:7318–7323

Lengke M, Fleet M, Southam G (2007) Biosynthesis of silver nanoparticles by filamentous cyanobacteria from a silver(I) nitrate complex. Langmuir 10:1021–1030

Li X, Xu H, Chen ZH, Chen G (2011) Biosynthesis of nanoparticles by microorganisms and their applications. J Nanomater 2011: 16. Article ID 270974. doi:10.1155/2011/270974

Liangwei D, Hong J, Xiaohua L, Erkang W (2007) Biosynthesis of gold nanoparticles assisted by *Escherichia coli* DH5α and its application on direct electrochemistry of hemoglobin. Electrochem Commun 9:1165–1170

Lin G, Tan DZ, Luo FF, Chen DP, Zhao QZ, Qiu JR (2011) Linear and nonlinear optical properties of glasses doped with Bi nanoparticles. J Non-Cryst Solids 357:2312–2315

Liu JH, Wang AQ, Chi YS, Lin HP, Mou CY (2005) Synergistic effect in an Au–Ag alloy nanocatalyst: CO oxidation. J Phys Chem B. 109:40–43

Liu X, Wang A, Li L, Zhang T, Mou CY, Lee JF (2013) Synthesis of Au–Ag alloy nanoparticles supported on silica gel via galvanic replacement reaction. Prog Nat Sci Mater Int 23:317–325

Lin, N, Huang J, Chang PR, Feng L, Yud J (2011) Effect of polysaccharide nanocrystals on structure properties and drug release kinetics of alginate-based microspheres. Colloids Surf B Biointerfaces 85:270–279

Lloyd JR, Yong P, Macaskie LE (1998) Enzymatic recovery of elemental palladium by using sulfate-reducing bacteria. Appl Environ Microbiol 64:4607–4609

Mahdieh M, Zolanvari A, Azimee AS, Mahdieh M (2012) Green biosynthesis of silver nanoparticles by *Spirulina platensis*. Scientia Iranica F 19:926–929

Malarkodi C, Rajeshkumar S, Vanaja M, Paulkumar K, Gnanajobitha G, Annadurai G (2013) Eco-friendly synthesis and characterization of gold nanoparticles using *Klebsiella pneumoniae*. J Nanostruct Chem 3:30

Mandal D, Bolander ME, Mukhopadhyay D, Sarkar G, Mukherjee P (2006) The use of microorganisms for the formation of metal nanoparticles and their application. Appl Microbiol Biotechnol 69:485–492

Mittal AK, Chisti Y, Banerjee UC (2013) Synthesis of metallic nanoparticles using plant extracts. Biotechnol Adv 31:346–356

Mo Z, Line P, Guo R, Deng Z, Zhao Y, Sun Y (2012) Graphene sheets/Ag 2S nanocomposites: synthesis and their application in super capacitor materials. Mater Lett 68:416–418

Mody VV, Siwale R, Singh A, Mody HR (2010) Introduction to metallic nanoparticles. J Pharm Bioallied Sci. 2:282–289

Mohampuria P, Rana N, Kumar Y (2008) Biosynthesis of nanoparticles: technological concepts and future applications. J Nanopart Res 10:507–517

Mousavi RA, Sepahy AA, Fazeli MR (2012) Biosynthesis, purification and characterization of cadmium sulfide nanoparticles using *Enterobacteriaceae* and their application. Proceedings of the International Conference Nanomaterials: Applications and Properties 1:5, Sumy State University, Alushta, The Crimea, Ukraine Kindly refer: http://essuir.sumdu.edu.ua/handle/123456789/34903.

Mubarak-Ali D, Sasikala M, Gunasekaran M, Thajuddin N (2011) Biosynthesis and characterization of silver nanoparticles using marine cyanobacterium *Oscillatoria willei* ntdm01. Dig J Nano Biostruct 6:385–390

Mukherjee P, Ahmad A, Mandal D, Senapati S, Sainkar SR, Khan MI, Ramani R, Parischa R, Ajayakumar PV, Alam M, Sastry M, Kumar R (2001a) Bioreduction of $AuCl_4^-$ ions by the fungus, *Verticillium* sp. and surface trapping of the gold nanoparticles formed. Angewandte Chemie—Int Ed. 40:3585–3588

Mukherjee P, Ahmad A, Mandal D, Senapati S, Sainkar SR, Khan MI, Parishcha R, Ajaykumar PV, Alam M, Kumar R, Sastry M (2001b) Fungus-mediated synthesis of silver nanoparticles and their immobilization in the mycelial matrix: a novel biological approach to nanoparticle synthesis. Nano Lett 1:515–519

Mukherjee P, Senapati S, Mandal D, Ahmad A, Khan MI, Kumar R, Sastry M (2002) Extracellular synthesis of gold nanoparticles by the fungus *Fusarium oxysporum*. ChemBioChem 3:461–463

Mukherjee P, Roy M, Mandal B, Dey G, Mukherjee P, Ghatak J, Tyagi AK, Kale SP (2008) Green synthesis of highly stabilized nanocrystalline silver particles by a non-pathogenic and agriculturally important fungus *Trichoderma asperellum*. Nanotechnology 19:75103–75110

Munusamy S, Bhakyaraj K, Vijayalakshmi L, Stephen A, Narayanan V (2016) Synthesis and characterization of cerium oxide nanoparticles using *Curvularia lunata* and their antibacterial properties. Int J Innovative Res Sci Eng. ISSN (Online) 2347–3207

Nair B, Pradeep T (2002) Coalescence of nanoclusters and formation of submicron crystallites assisted by *Lactobacillus* strains. Cryst Growth Des 2:293–298

Narayanan KB, Sakthivel N (2010) Biological synthesis of metal nanoparticles by microbes. Adv Colloid Interface Sci 156:1–13

Nazari P, Faramarzi MA, Sepehrizadeh Z, Mofid MR, Bazaz RD, Shahverdi AR (2012) Biosynthesis of bismuth nanoparticles using *Serratia marcescens* isolated from the Caspian Sea and their characterization. IET Nanobiotechnol 6:58–62

Ni YH, Yin G, Hong JM, Xu Z (2004) Rapid fabrication and optical properties of zinc sulfide nanocrystallines in a heterogeneous system. Mater Res Bull 39:1967–1972

Nies DH (2003) Efflux-mediated heavy metal resistance in prokaryotes. FEMS Microbiol Rev 27:313–339

Oremland RS, Herbel MJ, Switzer-Blum J, Langley S, Beveridge TJ, Ajayan PM, Sutto T, Ellis AV, Curran S (2004) Structural and spectral features of selenium nanospheres produced by Se-respiring bacteria. Appl Environ Microbiol 70:52–60

Pan J, Feng SS (2009) Targeting and imaging cancer cells by folate-decorated, quantum dots (QDs)-loaded nanoparticles of biodegradable polymers. Biomaterials 30:1176–1183

Pan R, Wua Y, Liew K (2010) Investigation of growth mechanism of nano-scaled cadmium sulfide within titanium dioxide nanotubes via solution deposition method. Appl Surf Sci 256: 6564–6568

Pan X, Ramirez IM, Mernaugh R, Liu J (2010) Nanocharacterization and bactericidal performance of silver modified titania photocatalyst. Colloids Surf B 77:82–89

Panacek A, Kvitek L, Procek R, Kolar M, Vecerova R, Pizurova N, Sharma VK, Nevěčná T, Zbořil R (2006) Silver colloid nanoparticles: synthesis, characterization, and their antibacterial activity. J Physical Chem B 110:16248–16253

Parikh RP, Singh S, Prasad BLV, Patole MS, Sastry M, Shouche YS (2008) Extracellular synthesis of crystalline silver nanoparticles and molecular evidence of silver resistance from *Morganella* sp.: towards understanding biochemical synthesis mechanism. ChemBioChem 9:1415–1422

Pearce CI, Coker VS, Charnock JM, Pattrick RAD, Mosselmans JFW, Law N, Beveridge TJ, Lloyd JR (2008) Microbial manufacture of chalcogenide-based nanoparticles via the reduction of selenite using *Veillonella atypica*: an in situ EXAFS study. Nanotechnology 19: 156603–156615

Peng D, Zhang J, Liu Q, Taylor EW (2007) Size effect of elemental selenium nanoparticles (Nano-Se) at supranutritional levels on selenium accumulation and glutathione S-transferase activity. J Inorg Biochem 101:1457–1463

Perez-Gonzalez T, Jimenez-Lopez C, Neal AL, Rull-Perez F, Rodriguez-Navarro A, Fernandez-Vivas A, Iañez-Pareja E (2010) Magnetite biomineralization induced by *Shewanella oneidensis*. Geochimicaet Cosmochimica Acta. 74:967–979

Prakash N, Sharma N, Prakash R, Raina K, Fellowes J, Pearce C, Lloyd J, Pattrick R (2009) Aerobic microbial manufacture of nanoscale selenium: exploiting nature's bio-nanomineralization potential. Biotechnol Lett 31:1857–1862

Prasad K, Jha AK (2010) Biosynthesis of CdS nanoparticles: an improved green and rapid procedure. J Colloid Interface Sci 342:68–72

Prasad K, Jha AK, Kulkarni AR (2007) *Lactobacillus* assisted synthesis of titanium nanoparticles. Nanoscale Res Lett 2:248–250

Qiao ZP, Xie Y, Qian YT, Zhu YJ (2000) g-Irradiation preparation and characterization of nanocrystalline ZnS. Mater Chem Phys 62:88–90

Qu J, Li G, Liu N, He J (2013) Preparation of $BiVO_4$/bentonite catalysts and their photocatalytic properties under simulated solar irradiation. Mater Sci Semicond Process 16:99–105

Rajeshkumar S, Malordi C, Vanaja M, Ghananajobitha G, Paulkumar K, Kannan C, Annadurai G (2013) Antibacterial activity of algae mediated synthesis of gold nanoparticles from *Turbinaria conoides*. Des Pharm Chem 5:224–229

Rajeshkumar S, Malarkodi C, Paulkumar K, Vanaja M, Gnanajobitha G, Annadurai G (2014) Algae mediated green fabrication of silver nanoparticles and examination of its antifungal activity against clinical pathogens. Int J Met. doi:10.1155/2014/692643, http://dx.doi.org/

Rangarajan V, Majumder S, Sen R (2014) Biosurfactant-mediated nanoparticles synthesis: a green and sustainable approach. In: Mulligan CN, Sharma SK, Mudhoo A (eds) Biosurfactants: research trends and applications. CRC Press Taylor & Francis Group, Boca Raton, Florida, pp 217–229

Reim N, Littig A, Behn D, Mews A (2013) Controlled electrodeposition of bismuth nanocatalysts for the solution—liquid—solid synthesis of CdSe nanowires on transparent conductive substrates. J Am Chem Soc 135:18520–18527

Rubilar O, Rai M, Tortella G, Diez MC, Seabra AB, Durán N (2013) Biogenic nanoparticles: copper, copper oxides, copper sulphides, complex copper nanostructures and their applications. Biotechnol Lett 35:1365–1375

Sahoo PK, Panigrahy B, Sahoo S, Satpati AK, Li D, Bahadur D (2013) In situ synthesis and properties of reduced grapheme oxide/Bi nanocomposites: as an electroactive material for analysis of heavy metals. Biosens Bioelectron 43:293–296

Saklani V, Jain VK (2012) Microbial synthesis of silver nanoparticles: a review. J Biotechnol Biomater S13:1–3

Sandoval A, Aguilar A, Louis C, Traverse A, Zanella R (2011) Bimetallic Au–Ag/$TiO_2$ catalyst prepared by deposition-precipitation: high activity and stability in CO oxidation. J Catal 281:40–49

Sanghi R, Verma P (2009) A facile green extracellular biosynthesis of CdS nanoparticles by immobilized fungus. Chem Eng J 155:886–891

Sastry M, Ahmad A, Khan I, Kumar R (2003) Biosynthesis of metal nanoparticles using fungi and actinomycete. Curr Sci 85:162–170

Sawle BD, Salimath B, Deshpande R, Bedre MD, Prabhakar BK, Venkataraman A (2008) Biosynthesis and stabilization of Au and Au-Ag alloy nanoparticles by fungus, *Fusarium semitectum*. Sci Technol Adv Mater 9:1–6

Schaffie M, Hosseini MR (2014) Biological process for synthesis of semiconductor copper sulfide nanoparticle from mine wastewaters. J Environ Chem Eng 2:386–391

Senapati S, Mandal D, Ahmad A, Mandal D, Senapati S, Sainkar SR, Khan MI, Parishcha R, Ajaykumar PV, Alam M, Kumar R, Sastry M (2004) Fungus mediated synthesis of silver nanoparticles: a novel biological approach. Indian J Phys A 78A:101–105

Senapati S, Ahmad A, Khan MI, Sastry M, Kumar R (2005) Extracellular biosynthesis of bimetallic Au-Ag alloy nanoparticles. Small 1:517–520

Shah R, Oza G, Pandey S, Sharon M (2012) Biogenic fabrication of gold nanoparticles using *Halomonas salina*. J Microbiol Biotechnol Res 2:485–492

Sharma VK, Yngard RA, Lin Y (2008) Silver nanoparticles: green synthesis and their antimicrobial activities. Adv Colloid Interface Sci 145:83–96

Sindhu R, Pandey A, Binod P (2015) Microbial diversity of nanoparticle biosynthesis. In: Singh O (ed) Bio-nanoparticles: biosynthesis and sustainable biotechnological implications, first edition. Wiley, New York, pp 187–203

Singaravelu G, Arockiamary JS, Kumar VG, Govindaraju K (2007) A novel extracellular synthesis of monodisperse gold nanoparticles using marine alga, *Sargassum wightii* Greville. Colloids Surf B 57:97–101

Singh S, Bhatta UM, Satyam PV, Dhawan A, Sastry M, Prasad BLV (2008) Bacterial synthesis of silicon/silica nanocomposites. J Mater Chem. 18:2601–2606

Sinha A, Khare SK (2011) Mercury bioaccumulation and simultaneous nanoparticle synthesis by *Enterobacter* sp. cells. Bioresour Technol 102:4281–4284

Slawson RM, Van Dyke MI, Lee H, Trevor JT (1992) Germanium and silver resistance, accumulation and toxicity in microorganisms. Plasmid 27:73–79

Southam G, Beveridge TJ (1996) The occurrence of sulfur and phosphorus within bacterially derived crystalline and pseudocrystalline octahedral gold formed in vitro. Geochim Cosmochim Acta 60:4369–4376

Sun Y, Xia YN (2002) Shape-controlled synthesis of gold and silver nanoparticles. Science 298:2176–2179

Suresh AK, Pelletier DA, Wang W, Broich ML, Moon JW, Gu B, Allison DP, Joy DC, Phelps TJ, Doktycz MJ (2011) Biofabrication of discrete spherical gold nanoparticles using the metal-reducing bacterium *Shewanella oneidensis*. Acta Biomater 7:2148–2152

Sweeney RY, Mao C, Gao X, Burt JL, Belcher AM, Georgiou G, Iverson BL (2004) Bacterial biosynthesis of cadmium sulfide nanocrystals. Chem Biol 11:1553–1559

Sweet MJ, Singleton I (2011) Silver nanoparticles: a microbial perspective. In: Advances in applied microbiology, 1st ed. ISBN: 978-0-12-3887044-5

Syed A, Ahmad A (2013) Extracellular biosynthesis of CdTe quantum dots by the fungus *Fusarium oxysporum* and their antibacterial activity. Spectrochim Acta Part A: Mol Biomol Spectrosc 106:41–47

Thakkar KN, Mhatre SS, Parikh RY (2009) Biological synthesis of metallic nanoparticles. Nanomed NBM 6:257–262

Tiquia SM (2008) Diversity of sulfate-reducing genes (*dsr*AB) in sediments from Puget Sound. Environ Technol 29:1095–1108

Tiquia SM, Gurczynski S, Zholi A, Devol A (2006) Diversity of biogeochemical cycling genes from Puget Sound sediments using DNA microarrays. Environ Technol 27:1377–1389

Torres SK, Campos VL, León CG, Rodríguez-Llamazares SM, Rojas SM, Gonzalez M, Smith C, Mondaca MA (2012) Biosynthesis of selenium nanoparticles by *Pantoea agglomerans* and their antioxidant activity. J Nanopart Res 14:1236

Tripathi RM, Bhadwal AS, Singh P, Shrivastav A, Singh MP, Shrivastav BR (2014) Mechanistic aspects of biogenic synthesis of CdS nanoparticles using Bacillus licheniformis. Adv Nat Sci: Nanosci Nanotechnol 5:025006

Tubtimtae A, Wu KL, Hao T, Lev MW, Wang GJ (2010) $Ag_2S$ quantum dot sensitized solar cells. Electrochem Commun 12:1158–1160

Vigneshwaran N, Kathe AA, Varadarajan PV, Nachane RP, Balasubramanya RH (2006) Biomimetics of silver nanoparticles by white rot fungus, *Phaenerochaete chrysosporium*. Colloids Surf B 53:55–59

Vigneshwaran N, Ashtaputre NM, Varadarajan PV, Nachane RP, Paralikar KM, Balasubramanya RH (2007) Biological synthesis of silver nanoparticles using the fungus *Aspergillus flavus*. Mater Lett 61:1413–1418

Wang FD, Buhro WE (2010) An easy shortcut synthesis of size controlled bismuth nanoparticles and their use in the SLS growth of high-quality colloidal cadmium selenide quantum wires. Small 6:573–581

Wang L, Cui ZL, Zhang ZK (2007) Bi nanoparticles and $Bi_2O_3$ nanorods formed by thermal plasma and heat treatment. Surf Coat Technol 201:5330–5332

Watson JHP, Ellwood DC, Soper AK, Charnock J (1999) Nanosized strongly-magnetic bacterially-produced iron sulfide materials. J Magn Magn Mater 203:69–72

Wei Y, Gin A, Razeghi M (2006) Quantum photovoltaic devices based on antimony compound semiconductors. Phys Astron 118:515–545

Wu W, Xiao XH, Zhang SF, Zhou JA, Fan LX, Ren F, Jiang CZ (2010a) Large-scale and controlled synthesis of iron oxide magnetic short nanotubes: shape evolution, growth mechanism, and magnetic properties. J Phys Chem C 114:16092–16103

Wu T, Zhou XG, Zhang H, Zhong XH (2010b) $Bi_2S_3$ nanostructures: a new photocatalyst. Nano Res 3:379–386

Wu W, Wu Z, Yu T, Jiang C, Kim WS (2015) Recent progress on magnetic iron oxide nanoparticles: synthesis, surface functional strategies and biomedical applications. Sci Technol Adv Mater 16: 023501 (43 p) doi:10.1088/1468-6996/16/2/023501

Xu C, Qu X (2014) Cerium oxide nanoparticle: a remarkably versatile rare earth nanomaterial for biological applications. NPG Asia Mater 6:e90. doi:10.1038/am.2013.88

Yacaman MJ, Ascencio JA, Liu HB, Gardea-Torresdey J (2001) Structure shape and stability of nanometric sized particles. J Vac Sci Technol B 19:1091–1103

Yadav V, Sharma N, Prakash R, Raina K, Bharadwaj LM, Prakas N (2008) Generation of selenium containing nanostructures by soil bacterium, *Pseudomonas aeruginosa*. Biotechnology 7:299–304

Yan S, Shen K, Xu X, Yi S, Wu J, Xiao X (2011) Formation Ag2S nanowires and Ag2S/CdS hetero structures via simple solvothermal route. Synth Met 161:1646–1650

Yang H, Santra S, Holloway PH (2005) Syntheses and applications of Mn-doped II-VI semiconductor nanocrystals. J Nanosci Nanotechnol 5:1364–1375

Yang YJ, Tao X, Hou Q, Chen JF (2009) Fluorescent mesoporous silica nanotubes incorporating CdS quantum dots for controlled release of ibuprofen. Acta Biomater 5:3488–3496

Ye C, Meng G, Zhang L, Wang G, Wang Y (2002) A facile vapour-solid synthetic route to $Sb_2O_3$ fibrils and tubules. Chem Phys Lett 363:34–38

Ye C, Wang G, Kong M, Zhang L (2006) Controlled synthesis of $Sb_2O_3$ nanoparticles, nanowires and nanoribbon. J Nanomater. Article ID 95670, 5 p

Yong P, Rowson NA, Farr JPG, Harris IR, Macaskie LE (2002a) Bioreduction and biocrystallization of palladium by *Desulfovibrio desulfuricans* NCIMB 8307. Biotechnol Bioeng 80:369–379

Yong P, Rowson NA, Farr JPG, Harris IR, Macaskie L (2002b) Bioaccumulation of palladium by *Desulfovibrio desulfuricans*. J Chem Technol Biotechnol 77:593–601

Zare B, Faramarzi MA, Sepehrizadeh Z, Shakibaie M, Rezaie S, Shahverdi AR (2012) Biosynthesis and recovery of rod-shaped tellurium nanoparticles and their bactericidal activities. Mat Res Bull. 47:3719–3725

Zhang W, Chena Z, Liua H, Zhang L, Gaoa P, Daping L (2011) Biosynthesis and structural characteristics of selenium nanoparticles by *Pseudomonas alcaliphila*. Colloids Surf B 88: 196–201

Zhang C, Zhang S, Yu L, Zhang Z, Zhang P, Wu Z (2012) Size controlled synthesis of monodisperse $Ag_2S$ nanoparticles by a solventless thermolytic methods. Mater Lett 85:77–80

Zhao Y, Zhang D, Shi W, Wang F (2007) A gamma ray irradiation reduction route to prepare rodlike $Ag_2S$ nanocrystallines at room temperature. Mater Lett 61:3232–3234

Zhou L, Wang WZ, Xu HL, Sun SM, Shang M (2009) $Bi_2O_3$ hierarchical nanostructures: controllable synthesis growth mechanism and their application in photocatalysis. Chem Eur J 15:1776–1782

Zheng D, Hu C, Gan T, Dang X, Hu S (2010) Preparation and application of a novel vanillin sensor based on biosynthesis of Au–Ag alloy nanoparticles. Sens Actuators B: Chem 148: 247–252